WIRELESS COMMUNICATIONS AND MOBILE COMPUTING
Wirel. Commun. Mob. Comput. 2003; **3**:663–685 (DOI: 10.1002/wcm.149)

Ultra-wideband wireless communications

Weihua Zhuang[1,*,†], Xuemin (Sherman) Shen[1] and Qi Bi[2]

[1]*Centre for Wireless Communications (CWC), Department of Electrical and Computer Engineering, University of Waterloo, Waterloo, Ontario N2L 3G1, Canada*
[2]*Lucent Technologies Inc., 67 Whippany Road, Whippany, New Jersey 07981, USA*

Summary

Ultra-wideband (UWB) communication techniques have attracted a great interest in both academia and industry in the past few years for applications in short-range wireless mobile systems. This is due to the potential advantages of UWB transmissions such as low power, high rate, immunity to multipath propagation, less complex transceiver hardware, and low interference. However, tremendous R&D efforts are required to face various technical challenges in developing UWB wireless systems, including UWB channel characterization, transceiver design, coexistence and interworking with other narrowband wireless systems, design of the link and network layers to benefit from UWB transmission characteristics. This paper is to provide an overview of UWB communications, summarize the previous research results, and identify further research issues that need to be tackled. The emphasis is placed on the commercial wireless communications. Copyright © 2003 John Wiley & Sons, Ltd.

KEY WORDS: call admission control (CAC); channel characterization; coexistence; medium access control (MAC); monocycle waveform; interworking; transceiver structure; ultra wideband (UWB) transmission

1. Introduction

Ultra-wideband (UWB) transmission is a widely used technology in radar and remote sensing applications [3] and has recently received great attention in both academia and industry for applications in wireless communications [5,37,38,41,75,79,94,97,116,117]. A UWB system is defined as any radio system that has a 10-dB bandwidth larger than 25 percent of its center frequency, or has a 10-dB bandwidth equal to or larger than 1.5 GHz if the center frequency is greater than 6 GHz [32]. The trends that drive recent R&D activities carried out for UWB transmission for commercial communication applications include [66]: (a) increasing demand for low-cost portable devices providing high-rate transmission capability at lower power than currently available, (b) lack of available frequencies, and crowding in currently assigned unlicensed frequency bands, (c) increasing availability of wireline high-speed Internet access in enterprises, homes and public places, and (d) decreasing semiconductor cost and power consumption for signal processing. Preliminary results demonstrate that UWB radio is a viable candidate for short-range multiple access communications in dense multipath environments. The preliminary approval of UWB

*Correspondence to: Weihua Zhuang, Centre for Wireless Communications (CWC), Department of Electrical and Computer Engineering, University of Waterloo, Waterloo, Ontario N2L 3G1, Canada.
†E-mail: wzhuang@bbcr.uwaterloo.ca
Contract/grant sponsor: Natural Science and Engineering Research Council (NSERC) of Canada; contract/grant numbers: RGPIN155131 and RGPIN203560.

technology made by Federal Communications Commission (FCC) of the United States reserves the frequency band between 3.1 and 10.6 GHz for indoor UWB communication systems [32]; however, most of the works reported in the open literature so far were carried out before the FCC approval. As a result, the frequency bands of some UWB transmission schemes presented in this paper go beyond the FCC limits. In general, UWB technology has many benefits due to its ultra-wideband nature, which include the following:

1. *High data rate*—UWB technology is likely to provide high data rates in short- and medium-range (such as 20 m, 50 m) wireless communications [75];
2. *Less path loss and better immunity to multipath propagation*—As UWB spans over a very wide frequency range (from very low to very high), it has relatively low material penetration losses. On the other hand, UWB channels exhibit extremely frequency-selective fading, and each received signal contains a large number of resolvable multipath components [115,118]. The fine-time resolution of UWB signals facilitates the receiver to coherently combine multipath signal components with path length differentials down to about 30 cm [70].[1] The carrier-less nature of UWB signals results in less fading, even when pulses overlap. This reduces fade margin in link budgets [111,118];
3. *Availability of low-cost transceivers*—The transceiver structure may be very simple due to the absence of the carrier. The techniques for generating UWB signals have existed for more than three decades [90]. Recent advances in silicon process and switching speeds make commercial low-cost UWB systems possible [35,38,46,64,65,102].
4. *Low transmit power and low interference*—For a short-range operation, the average transmit power of pulses of duration on the order of one nanosecond with a low duty cycle is very low. With an ultra-wideband spectrum bandwidth, the power spectral density of UWB signals is extremely low. This gives rise to the potential that UWB systems can coexist with narrowband radio systems operating in the same spectrum without causing undue interference. Also, UWB operates with emission levels commensurate with common digital devices such as laptop computers, palm Pilots, and pocket calculators. It may further utilize the frequency spectrum used by existing services.

On the other hand, there exist many technical challenges in UWB deployment. These include: (a) distortion of the received waveform from each distinct delayed propagation path, which makes it difficult to explore path diversity inherent in the received signal [17]; (b) synchronization of very short pulses at the receiver; (c) performance degradation due to multiple access interference and narrowband jamming; (d) employing higher order modulation schemes to improve capacity or throughput; (e) development of link and network layers to take advantage of the UWB transmission benefits at the physical layer.

UWB technology has potentials for applications in communications, radar and location [1,37,39,40,97]. In recent years, R&D efforts have resulted in advances of UWB technology in areas such as antennas [31,52,92,102], power amplifiers [60], timing chips and synchronizers [33,59]. For wireless communications in particular, the applications and hardware that have been developed and demonstrated in the past few years include the following [37,97,109]: (a) For short range operation up to 5 m, data rates up to 600 Mbps are possible within the limits specified in the Code of Federal Regulations for intentional radiators [107] while introducing only negligible interference to coexisting users; (b) At a range of 10 m with an effective average output power of 50 μW, a simplex 2.0 GHz data link can support a data rate of 5 Mbps at less than 10^{-8} bit error rate without forward error correction; (c) At a range of 1–2 km, a full duplex 1.5 GHz handheld radio unit provides a data rate of up to 128 kbps with an average output power of 640 μW; (d) At a range beyond 16 km, a full duplex 1.3 GHz radio system has a variable data rate of either 39 kbps or 156 kbps with an average output power of 250 μW. In addition, a highly mobile, multimode, ad hoc wireless communication network based on UWB technology is under development to provide a secure, low probability of intercept and detection, and to support encrypted voice/data (up to 128 kbps) and high-rate

[1]This approach to mitigating channel impairments is totally different from some techniques used in narrowband systems. For example, a basic approach to combating frequency-selective fading in high-rate narrowband systems is to partition the signal into contiguous frequency bands, each of which is narrow compared with the coherence bandwidth of the channel. Each of the signal components is then modulated onto a different subcarrier and the signal components are sent over the channel in parallel. In this way, each of the signal components experiences frequency flat fading. This can be achieved by converting the high rate serial data sequence into a number of lower rate parallel sequences and then modulating each onto a subcarrier. An effective method to achieve this is orthogonal frequency division multiplexing (OFDM).

video (1.544 Mbps T1) transmissions. In general, there is a tradeoff between the average power (and correspondingly the distance) and data rate. For short distance transmission, such as in an indoor wireless system or a home entertainment network [124], UWB technology has the potential to enable simple, low-cost and high-rate applications such as digital video; as the distance increases, UWB wireless systems are likely to support a data rate such as 20 Mbps in local area and wide area networks (LAN/WANs).

Even though R&D results so far have demonstrated that UWB radio is a promising solution for high-rate short-range wireless communications, further extensive investigation, experiment, and development are necessary towards developing effective and efficient UWB communication systems and developing UWB technology. This paper is to make a contribution to the development of UWB systems.[2] It provides an overview of UWB communications, summarizes the previous research results, and identifies further work that should be looked into. The emphasis is placed on the commercial wireless communications. This paper is organized as follows: Section 2 describes the principles of UWB transmission, including impulse radio (IR) using pulse position modulation (PPM) and pulse amplitude modulation (PAM). In Section 3, we present some existing models for the UWB radio channel based on preliminary experiments. Receiver structures and their performance are discussed in Section 4. Section 5 is devoted to resource allocation issues at the link layer (for medium access control) and network layer for quality-of-service (QoS) provisioning, followed by conclusions in Section 6.

2. UWB Transmission

UWB usually refers to *impulse* based waveforms that can be used with different modulation schemes. The transmitted signal consists of a train of very narrow pulses at baseband, normally on the order of a nanosecond. Each transmitted pulse is referred to as a *monocycle*. The information can be carried by the position or amplitude of the pulses. In general, narrower pulses in the time domain correspond to electromagnetic radiation of wider spectrum in the frequency domain. Thus, the baseband train of nanosecond impulses can have a frequency spectrum spanning from zero to several GHz, resulting in the so called UWB transmission.

2.1. Monocycle Waveforms

The frequency-domain spectral content of a UWB signal depends on the pulse waveform shape and the pulse width. Typical pulse waveforms used in research include rectangular, Gaussian, Gaussian doublet, and Rayleigh monocycles, etc. [11,17,44,93,125]. A monocycle should have zero DC component to allow it to radiate effectively. In fact, to satisfy the UWB emission constraint specified in FCC regulation 47 CFR Section 15.5(d), the desired frequency spectrum of the monocycle waveform should be flat over a target bandwidth not including the zero frequency.

A rectangular monocycle with width T_p and unity energy can be represented by $\sqrt{\frac{1}{T_p}}[U(t) - U(t - T_p)]$, where $U(\cdot)$ denotes the unit step function. The rectangular pulse has a large DC component, which is not a desired property. Even so, the rectangular monocycle has often been used in academic research because of its simplicity.

A generic Gaussian pulse is given by

$$p_g(t) = \frac{1}{\sqrt{2\pi}\sigma}\exp\left[-\frac{1}{2}\left(\frac{t-\mu}{\sigma}\right)^2\right] \qquad (1)$$

where μ defines the center of the pulse and σ determines the width of the pulse. Some popular monocycles are derived from the Gaussian pulse. The Gaussian monocycle is the second derivative of a Gaussian pulse, and is given by

$$p_G(t) = A_G\left[1 - \left(\frac{t-\mu}{\sigma}\right)^2\right]\exp\left[-\frac{1}{2}\left(\frac{t-\mu}{\sigma}\right)^2\right] \qquad (2)$$

where the parameter σ determines the monocycle width T_p. The effective time duration of the waveform that contains 99.99% of the total monocycle energy is $T_p = 7\sigma$ centered at $\mu = 3.5\sigma$. The factor A_G is introduced so that the total energy of the monocycle is normalized to unity, i.e. $\int p_G^2(t)\mathrm{d}t = 1$. The frequency spectrum of the Gaussian monocycle is

$$P_G(f) = A_G\sqrt{2\pi}\sigma(2\pi\sigma f)^2\exp\left[-\frac{1}{2}(2\pi\sigma f)^2\right] \times \exp(-j2\pi f\mu)$$

[2] In this paper, narrowband transmission refers to non-UWB transmission, which includes conventional wideband transmission such as wideband code-division multiple access (CDMA) transmission in the third-generation cellular systems.

The Gaussian doublet is a bipolar signal, consisting of two amplitude reversed Gaussian pulses with a time gap of T_w between the two pulses. The mathematical expression for the monocycle is

$$p_{GD}(t) = A_{GD}\left\{\exp\left[-\frac{1}{2}\left(\frac{t-\mu}{\sigma}\right)^2\right] - \exp\left[-\frac{1}{2}\left(\frac{t-\mu-T_w}{\sigma}\right)^2\right]\right\} \quad (3)$$

which has a Fourier transform given by

$$P_{GD}(f) = 2A_{GD}\sqrt{2\pi}\sigma\,\sin(\pi f T_w)\,\exp\left[-\frac{1}{2}(2\pi\sigma f)^2\right] \times \exp\{-j[2\pi f(\mu + 0.5T_w) - 0.5\pi]\}$$

The pulse width is determined by the parameters μ, σ, and T_w. The truncated pulse with $T_p = 14\sigma$ for $T_w = 7\sigma$ contains 99.99% of the total monocycle energy.

The Rayleigh monocycle is derived from the first derivative of the Gaussian pulse and is given by

$$p_R(t) = A_R\left[\frac{t-\mu}{\sigma^2}\right]\exp\left[-\frac{1}{2}\left(\frac{t-\mu}{\sigma}\right)^2\right] \quad (4)$$

with the Fourier transform

$$P_R(f) = A_R\sqrt{2\pi}(2\pi\sigma f)\,\exp\left[-\frac{1}{2}(2\pi\sigma f)^2\right] \times \exp[-j(2\pi f\mu + 0.5\pi)]$$

The effective time duration of the waveform that contains 99.99% of the total monocycle energy is $T_p = 7\sigma$ centered at $\mu = 3.5\,\sigma$, which is the same as that of the Gaussian monocycle.

Different from the rectangular waveform, an important feature of the above monocycles is that they do not have a DC component, which makes the radiation of the monocycles more efficient. Figure 1 shows the UWB monocycles and their frequency spectra in dB, where the maximum magnitudes of the monocycles and spectra are normalized to unity and 0 dB respectively. Define the 10-dB bandwidth of the monocycles as $B_{10\text{dB}} = f_H - f_L$, where f_H and f_L are the frequencies at which the magnitude spectrum attains $1/\sqrt{10}$ of its peak value, and the nominal center frequency as $f_c = (f_H + f_L)/2$. Table I lists the 10-dB bandwidth and center frequency for the monocycles, where

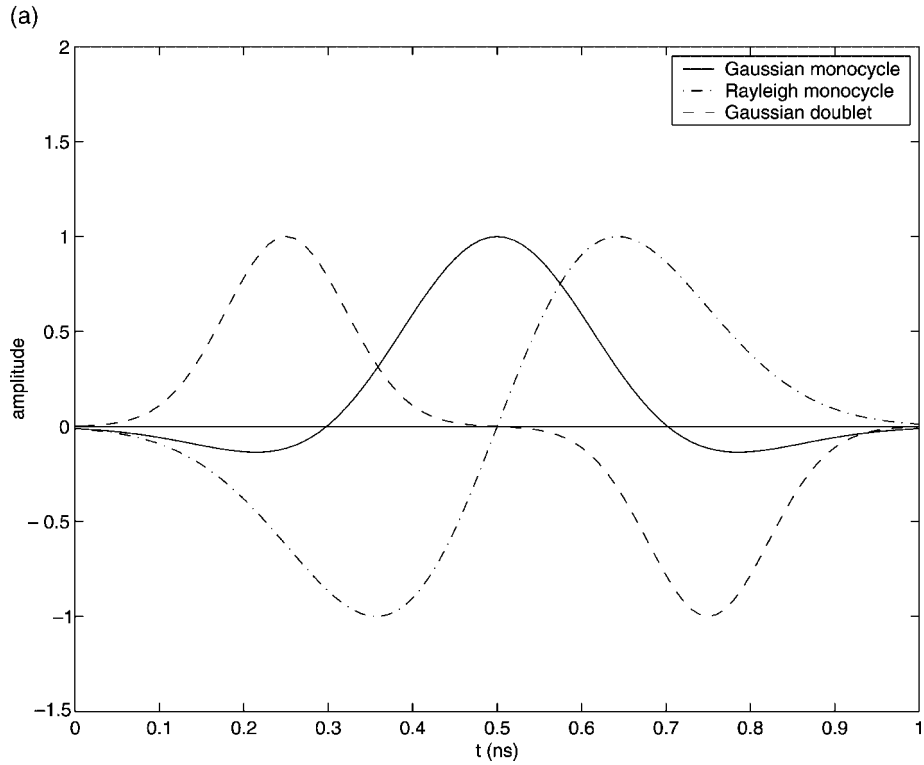

Fig. 1. The waveforms and magnitude spectra of Gaussian monocycle, Rayleigh monocycle, and Gaussian doublet with $T_p = 1$ ns and $T_w = 0.5$ ns; (a) Monocycle waveforms; (b) Magnitude spectra.

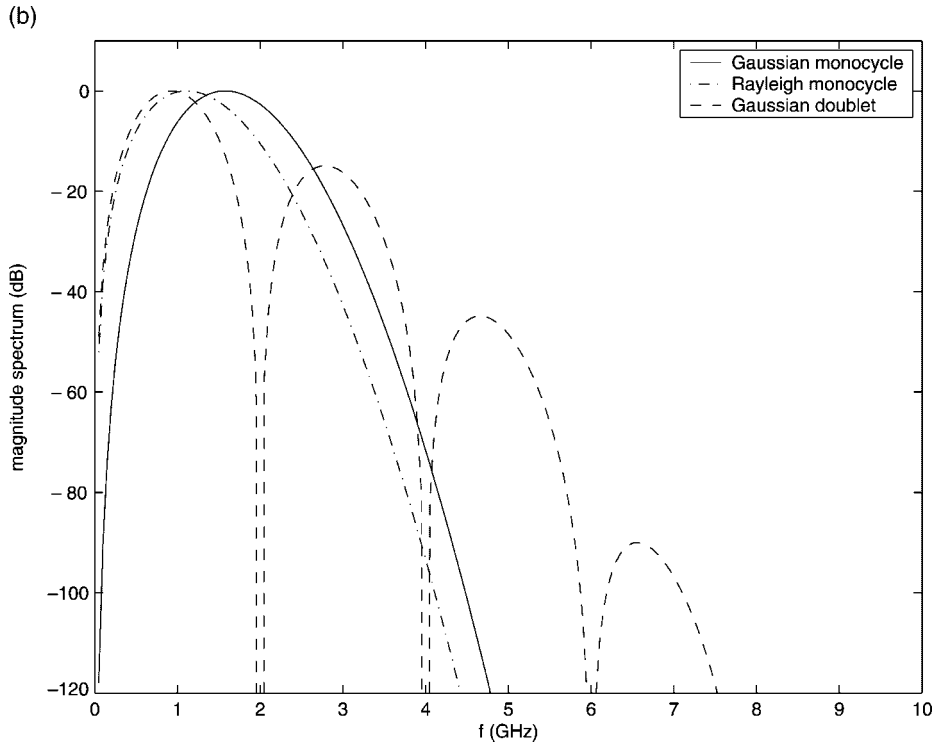

Fig. 1. Continued

Table I. The 10-dB bandwidth and center frequency of the monocycles.

Monocycle	$B_{10\,\mathrm{dB}}$	f_c
Gaussian	$1.11/T_p$	$1.61/T_p$
Rayleigh	$1.11/T_p$	$1.16/T_p$
Gaussian doublet	$0.83/T_p$	$0.94/T_p$

$T_w = T_p/2$ for the Gaussian doublet. Note that the Gaussian doublet has a larger out-band radiation than the other two monocycles, even though it has a smaller 10-dB bandwidth.

Important criteria in designing the monocycle waveform include (a) simplicity of the monocycle generator and (b) minimal interference between the UWB system and other narrowband systems coexisting in the same frequency band (as to be discussed later in this section).

2.2. Modulation

The two most popular UWB transmission models are based on the concepts of time hopping spread spectrum (TH-SS) and direct sequence spread spectrum (DS-SS) respectively. Data information can be modulated to the UWB impulse train using pulse position modulation (PPM) or pulse amplitude modulation (PAM).[3] For simplicity, consider binary modulation. In both TH-SS and DS-SS UWB models, one information bit is spread over multiple monocycles to achieve a processing gain in reception.

In order to represent the transmitted signals, the following mathematical symbols are introduced:

T_f—the nominal pulse repetition interval
T_c—chip interval
N_s—the number of monocycles modulated by each information bit, referred to as spreading factor
T_d—bit interval, equal to $N_s T_f$ in TH-SS and to $N_s T_c$ in DS-SS
$\{c_d\}$—a binary pseudorandom noise (PN) code sequence of length N_s in DS-SS, $c_d \in \{-1, +1\}$

[3]Here we consider binary antipodal PAM. Note that phase modulation in general is not applicable to UWB transmission due to its carrier-less nature.

$\{c_t\}$—a binary PN code sequence for TH, which defines unique code phases in the interval $[0,\ N_t]$ where $N_t T_c < T_f$ and $c_t \in \{0,\ 1\}$

j—chip index of the PN sequence

$\{d_n\}$—information data sequence, $d_n = 0$ for symbol "1" and $d_n = 1$ for symbol "0" in PPM, and $d_n = 1$ for symbol "1" and $d_n = -1$ for symbol "0" in PAM

δ—an extra delay of monocycles for symbol "0" in PPM

n—information bit index

$p(t)$—monocycle waveform, examples including those given in Equations (2), (3) and (4)

E_p—monocycle energy

The transmitted signal in TH-SS using PPM is given by

$$x(t) = \sqrt{E_p} \sum_{n=1}^{\infty} \sum_{j=0}^{N_s-1} p[(t - nT_d - jT_f - (c_t)_j T_c - \delta d_n)] \tag{5}$$

with the energy of the pulse $p(t)$ being unity. On a large scale, the time is partitioned to frames of bit interval T_d. Within each frame, there are N_s monocycles. Each monocycle experiences a distinct extra delay $(c_t)_j T_c$ different from the rest of the monocycles within the frame in order to avoid catastrophic collisions in multiple access. Depending on the information bit, all the monocycles in the frame experience an extra common delay $\delta(>0)$ for information symbol '0'. The ratio $N_t T_c / T_f$ represents the percentage of time in each frame over which TH is allowed. The ratio should not be too small in order to avoid catastrophic collisions. Similarly, the transmitted signal in DS-SS using PPM is given by

$$x(t) = \sqrt{E_p} \sum_{n=1}^{\infty} \sum_{j=0}^{N_s-1} (c_d)_j p(t - nT_d - jT_f - \delta d_n) \tag{6}$$

The DS-SS PPM is also referred to as hybrid DS-TH UWB [56]. Here, we consider orthogonal PPM where all the monocycles do not overlap, i.e. $\delta \geq T_p$ in Equations (5) and (6).

Correspondingly, using PAM, the transmitted signal is

$$x(t) = \sqrt{E_p} \sum_{n=1}^{\infty} \sum_{j=0}^{N_s-1} p[t - nT_d - jT_f - (c_t)_j T_c] d_n \tag{7}$$

in TH-SS and is

$$x(t) = \sqrt{E_p} \sum_{n=1}^{\infty} \sum_{j=0}^{N_s-1} (c_d)_j p(t - nT_d - jT_f) d_n \tag{8}$$

in DS-SS. In summary, the transmitted signal can be represented as

$$x(t) = \sqrt{E_p} \sum_{n=1}^{\infty} \sum_{j=0}^{N_s-1} p_t(t - nT_d - jT_f) \tag{9}$$

where the modulated monocycle $p_t(t)$ is a function of j and n, and is given by

$$p_t(t) = \begin{cases} p[t - (c_t)_j T_c - \delta d_n] & \text{(TH-SS PPM)} \\ (c_d)_j p(t - \delta d_n) & \text{(DS-SSP PM)} \\ p[t - (c_t)_j T_c] d_n & \text{(TH-SS PAM)} \\ (c_d)_j p(t) d_n & \text{(DS-SS PAM)} \end{cases} \tag{10}$$

The transmission data rate R_s in bps is equal to $1/(N_s T_f)$ in TH-SS and to $1/(N_s T_c)$ in DS-SS. Given the spreading factor N_s, the information data rate R_s depends on the pulse repetition interval T_f or the chip interval T_c.

Figure 2 shows the difference between TH-SS and DS-SS [44], where PAM is used for illustration clarity. A similar illustration can be drawn for PPM. From the figure, the following observations can be made:

1. In DS-SS PAM, we have $T_c = T_p = T_f$, leading to a duty cycle of 100%. The DS-SS PAM is basically DS-CDMA using BPSK (binary phase shift keying) except that the carrier frequency is zero and the chip pulse is the UWB monocycle. Within each frame, the information bit is to modulate N_s evenly distributed (in the time axis) monocycles and each PN code chip is to determine the polarity (positive or negative) of the corresponding monocycle after the data modulation. Signals for different users are to be separated through PN code correlation as in DS-CDMA;
2. The power spectral density (psd) of the above UWB signals can be calculated using the mathematical expressions given in Reference [114]. In DS-SS PAM, with a constant T_f, line spectrum appears in the frequency domain and the separation between the adjacent lines is proportional to $1/T_f$. The spectrum lines are not desired as they can introduce noticeable interference to other radio

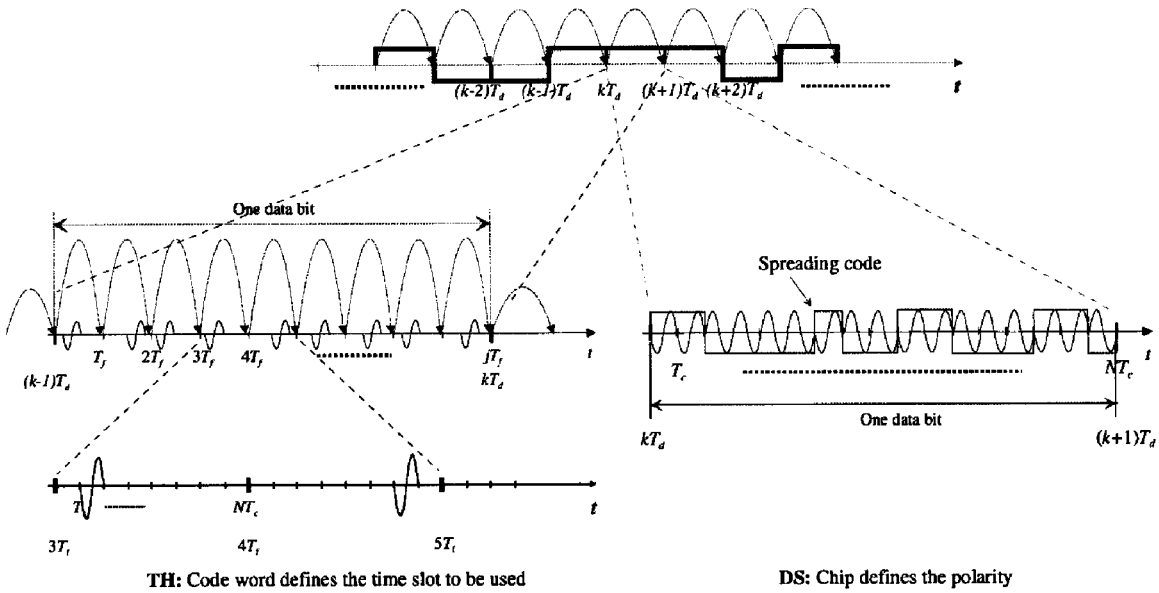

Fig. 2. Comparison of TH-SS PAM and DS-SS PAM waveforms [©2002 IEEE. Reproduced from Hämäläinen M, *et al.* On the UWB system coexistence with GSM 900, UMTS/WCDMA and GPS. *IEEE Journal on Selected Areas in Communications* 2002; **20**(9): 1712–1721. DOI: 10.1109/JSAC.2002.805242, by permission of the IEEE.]

systems in the same frequency spectrum. This is a drawback of DS-SS PAM as compared with the other three schemes where the monocycles are not evenly distributed in each frame;

3. In the other three schemes (TH-SS PPM, DS-SS PPM, and TH-SS PAM), $T_f \geq N_t T_c$ and $T_c \geq T_p$, leading to a very small duty cycle (i.e., $T_p/T_f \ll 1$). Given the same monocycle width T_p, T_f in DS-SS PAM is much smaller than that in the other three schemes. As a result, the information rate R_s in DS-SS PAM is much higher than that in the other cases when the T_p and N_s values are the same for all the four schemes;
4. For the same spreading factor N_s and information data rate R_s, the repetition interval T_f and the number of monocycles within each frame (bit interval) are the same among all the four schemes. However, the DS-SS PAM scheme has a much larger monocycle width T_p (with a duty cycle of 1) than that in the other schemes (with a duty cycle much smaller than 1), leading to a small ratio of peak power to average power and an overall smaller bandwidth;
5. The psd mainly depends on the width and waveform of the monocycle and on whether TH-SS or DS-SS is used. Based on the application, the monocycle waveform can be designed for minimum interference at certain frequency bands;
6. In TH-SS PPM, all the monocycles have the same polarity and the modulation is achieved completely by time shifting of monocycles, which is not the case in the other schemes. Therefore, early research on UWB for wireless communications focused on TH-SS PPM due to its implementation advantage of not requiring pulse inversion [93,116,117].

In Equations (5), (7) and (8), it is assumed that the PN sequences are periodic with period N_s for simplicity of presentation. Also, higher order modulation (such as M-ary PPM and other M-ary orthogonal modulation) is possible [28,86,123], which achieves a higher throughput at the expense of implementation complexity and transmission accuracy.

In addition to using UWB monocycles in the conventional UWB transmission, UWB systems using narrowband signals have been explored as a design alternative [24,121]. In Reference [121], UWB based on the well-known family of frequency-hopping (FH)-SS multiple access technique is proposed, where multistage FH multiple access, the associated spectrum assignment and the residue number system (RNS) based FH strategy are investigated and proposed. The UWB based on the conventional narrowband signalling has the advantages of exploring numerous well-understood and spectral-efficient techniques originally developed for narrowband signalling in order to achieve high transmission efficiency, in addition to using elements of the existing standards. In Reference [24] multi-bands UWB is proposed, where

each UWB signal occupies 500 MHz of spectrum and does not have to be an impulse train. The approach is adaptive and scalable, and is flexible in accommodating various transmission rate requirements. Interference mitigation techniques should be developed to protect existing narrowband systems in UWB interfering with narrowband and to ensure that UWB is robust in narrowband interfering with UWB.

2.3. UWB Coexistence

As UWB systems will coexist with other existing narrowband systems/standards in the same frequency spectrum, how UWB transmission and narrowband transmission interfere with each other is an important issue to ensure that both these systems operate properly in the mutual interference. The information will help to design UWB systems for a minimum mutual interference. Initial investigation has been carried out and reported in References [44,45,125] for a correlator receiver in an additive Gaussian white noise (AWGN) channel. The coexistence issue of UWB systems using TH-SS PAM and DS-SS PAM (with the same bit energy and spreading factor) has been investigated via computer simulations [44,45], where the narrowband systems include GSM900, UMTS/WCDMA and GPS.[4] It is concluded that the mutual interference can be reduced by properly designing the monocycle waveform and properly choosing its width. In terms of the interference from UWB systems to the narrowband systems, it is observed that: (a) UWB systems cause less interference to the frequency spectra of the narrowband systems when higher order Gaussian waveforms are used (up to the third derivative of the Gaussian pulse is considered); (b) in the GPS L1 and L2 channels, DS-SS UWB introduces less interference than TH-SS UWB; (c) both TH-SS and DS-SS UWB systems generate a similar level of interference in GSM900 and UMTS/WCDMA bands. As to the UWB transmission performance degradation due to jamming from the narrowband systems, it is observed that: (a) the UWB transmission performance suffers most when the interferer spectrum overlaps with the nominal center frequency of the UWB systems. Thus, the UWB monocycle waveform and bandwidth should be designed carefully to reduce interference from a given band; (b) TH-SS UWB outperforms DS-SS UWB at a low interference level; (c) both TH-SS and DS-SS UWB systems have similar performance at a high jamming power level. In Reference [125], the effect of narrowband jamming on TH-SS PPM systems using rectangular pulse, Gaussian and Rayleigh monocycles is analyzed. It is demonstrated that, comparing with narrowband DS-SS with Gaussian chip waveform, the UWB system using Gaussian monocycle has a significant advantage in suppressing both narrowband and wideband interference.

Further investigation on the interference for UWB system coexistence is necessary for more practical UWB channels using a rake receiver, and in the presence of multiple access interference using an optimal or suboptimal receiver (see Section 4 for more details of the receivers). Also, the effect of narrowband jamming at multiple bands on UWB transmission performance should be studied.

3. Channel Characterization

Accurate channel characterization is vital for UWB transceiver design and for efficient utilization of the system resources (such as frequency spectrum and transmit power), as the propagation channel sets fundamental limits on the performance of UWB communication systems. Due to reflection, refraction and scattering, wireless signals usually experience multipath propagation. In a narrowband system, this phenomenon leads to multipath fading, while in UWB systems the monocycles often do not overlap because the pulse width is often smaller than the channel propagation delays. Extensive work has been done in the characterization of the narrowband indoor propagation channel [47]. Given the wideband nature of UWB transmission, the conventional channel models developed for narrowband transmissions are not adequate for UWB transmission. So far, only very limited measurement results and preliminary investigation on the channel modelling are available in the open literature for UWB transmission [8,21,29, 53,84,113,115,117,119,122]. In the following, we first discuss UWB channel statistics and models based on the measurements, and then present some attempts to model the UWB channel using theoretical tools.

3.1. Large-Scale Path Loss

In wireless systems, as the distance between the transmitter and receiver increases, the received signal

[4]GSM stands for Global System for Mobile Communications, UMTS for Universal Mobile Telecommunications Service, and GPS for Global Positioning System

becomes weaker because of the growing propagation attenuation with the distance. Large-scale path loss characterizes the local average of the path loss. The log-distance path loss model is a popular choice for narrowband systems in both indoor and outdoor cellular environments [47,89]. Preliminary measurement results indicate that the model is also valid for UWB indoor propagation [8,122]. Let $\bar{L}_p(d)$ denote the log-distance path loss, which is a function of the distance d separating the transmitter and the receiver. Then,

$$\bar{L}_p(d) \propto \left(\frac{d}{d_0}\right)^{\kappa}, \qquad d \geq d_0 \tag{11}$$

or equivalently,

$$\bar{L}_p(d) = \bar{L}_p(d_0) + 10\kappa \log_{10}\left(\frac{d}{d_0}\right) \text{dB}, \qquad d \geq d_0 \tag{12}$$

where κ is the path loss exponent and d_0 is the close-in reference distance. A typical value for d_0 is 1 m for indoor systems [8,89]. Analysis of the measurement data from a modern laboratory/office building [8] indicates that the $\kappa = 2.04$ for $d \in [1,11]$ m and $\kappa = 7.4$ for $d > 11$ m. The measurement data collected from a single-floor, hard-partition office building (fully furnished) of recent construction [122] show that $\kappa = 2.9$ for the peak received power, $\kappa = 2.1$ for the total received power, and $\kappa = 2.5$ when using a 4-finger rake (referred to as peak plus rake) receiver locking to the strongest paths. This suggests that receiver architectures should make use of the total received power in order to combat path loss more effectively. In comparison, the path loss exponent value of the UWB channels is smaller than that of narrowband systems (where $\kappa = 2.68 \sim 4.33$ [89] and $\kappa = 3 \sim 4$ [42]).

3.2. Lognormal Shadowing

As the receiver moves in an indoor environment, it often travels into a propagation shadow behind obstacles much larger than the wavelength of the transmitted signal and therefore, experiences a severe attenuation of the received signal power. This phenomenon is called shadowing. A lognormal distribution is often used to characterize the shadowing process in narrowband systems [47,89] and is assumed for UWB transmission [8]. As a result, large-scale path loss is a combination of log-distance path loss and lognormal shadowing. Let $\epsilon_{(\text{dB})}$ represent the shadowing effect, which is a zero-mean Gaussian distributed random variable (in dB) with standard deviation σ_ϵ (in dB). Measurements indicate that σ_ϵ is 4.3 dB [8], and is 4.75 dB, 4.04 dB and 3.55 dB for the peak, peak plus rake and total received power respectively [122]. The values are in general smaller than the typical value ($4.3 \sim 13.3$ dB [89] and $6 \sim 12$ dB [42]) of narrowband systems, suggesting that a relatively small fading margin is required for UWB transmission.

The *signal quality* in dB is defined as

$$Q(u) = 10\log_{10} E_{\text{tot}}(u) - 10\log_{10} E_{\text{ref}} \tag{13}$$

where E_{tot} is the received energy at a specific measurement position u and E_{ref} is the reference energy chosen to be the energy in the line-of-sight (LOS) path measured by the receiver located at d_0 ($= 1$ m). Measurement data given in Reference [119] show that the received signal energy varies by at most 5 dB as the receiver position changes over the measurement grid within a room having 49 measurement points on a 7×7 square grid with 6-inch spacing. Compared with the fading margin in narrowband systems (such as 20–30 dB reported in Reference [72]), the variation in the received signal energy is very small. Again, this indicates the potential of UWB radio for robust indoor communications at a low transmit power level.

3.3. Small-Scale Fading Characteristics

Analysis shows that the well-established tapped-delay-line channel model with independently faded tap (bin) gains for narrowband systems [91] is also valid for UWB transmission [8,20]. The power delay profile is an exponential function of the excess delay, with the decay constant (in a dB scale with reference value of 1 ns) following the lognormal distribution with mean 16.1 and standard deviation 1.27. Also, the power ratio of the first path to the second path follows the lognormal distribution with mean -4 and standard deviation 3. Different from the narrowband channel models, the energy statistics due to small-scale effects follow a Gamma distribution $\Gamma(\Omega, m)$ with parameters Ω and m for all bins. The parameter m is a random variable following a truncated Gaussian distribution given by

$$f_m(x) = \begin{cases} K_m \exp\left[-\frac{(x-\mu_m)^2}{2\sigma_m^2}\right], & x \geq 0.5 \\ 0, & x < 0.5 \end{cases} \tag{14}$$

denoted by $m \sim \mathcal{T}_{\mathcal{N}}(\mu_m, \sigma_m^2)$, where K_m is chosen so that $\int_{-\infty}^{\infty} f_m(x)\mathrm{d}x = 1$. Let $\tau_l = 2(l-1)$ ns, denoting the excess delay of the lth bin, then the parameters μ_m and σ_m^2 as a function of τ_l are given by

$$\mu_m(\tau_l) = 3.5 - (\tau_l/73)$$
$$\sigma_m^2(\tau_l) = 1.84 - (\tau_l/160)$$

The linear tapped-delay-line model is also used in the data post-processing reported in [53], where the Rician fading model is assumed for each tap gain. Each complex tap gain contains a deterministic component (s_{dB}^2) from the LOS path and a random component (η_{dB}^2) from NLOS paths, and the k-factor in logarithmic scale of the Rician distribution is denoted by k ($= s_{\mathrm{dB}}^2 - \eta_{\mathrm{dB}}^2$). The k-factor is a function of the propagation delay τ and the transmitter-receiver distance d. A linear regression line

$$\begin{aligned} k(\tau, d) &= a(\tau)d + b(\tau) \\ &= [a_s(\tau) - a_\eta(\tau)]d + [b_s(\tau) - b_\eta(\tau)] \end{aligned}$$

can be fitted to the k-factor normalized to the average power level, where d is the logarithmic antenna separation, and subscripts s and η are associated with s_{dB}^2 and η_{dB}^2 respectively. At $\tau = 0$, $a(\tau) \approx 0$ and, at $\tau = 5$ ns, $a(\tau) = -1.67$. Piecewise linear regression lines also apply to the parameters a_s, a_η, b_s, and b_η, given by

$$a_s(\tau) = \alpha_s'\tau + \alpha_s$$
$$a_\eta(\tau) = \alpha_\eta'\tau + \alpha_\eta$$
$$b_s(\tau) = \beta_s'\tau + \beta_s$$
$$b_\eta(\tau) = \beta_\eta'\tau + \beta_\eta$$

Table II lists the values for the exponential decay coefficients extracted from the measurement data.

Table II. Parameters for exponential decay coefficients α and β [53].

τ (ns)	α_s' (dB)	α_s (dB)	τ (ns)	α_η' (dB)	α_η (dB)
$0 \sim 6$	-0.095	-1.20	$0 \sim 28$	0.0	-0.42
$6 \sim 60$	0.035	-1.98	$28 \sim 60$	0.015	-0.84
τ (ns)	β_s' (dB)	β_s (dB)	τ (ns)	β_η' (dB)	β_η (dB)
$0 \sim 10$	-0.00	-15.2	$0 \sim 28$	0.00	-42.7
$10 \sim 60$	-0.47	-10.6	$28 \sim 60$	-0.15	-38.5

The root-mean-square (rms) delay spread increases with the distance between the transmitter and receiver, because the propagation paths become more nonuniform as the distance increases [122]. Also, the rms delay increases with the path loss, likely due to the earliest arriving multipath components being attenuated and not dominating the delay spread over the later arriving components. The rms delay spread is 5.72 ns and 4.26 ns versus distance (ranging approximately from 1 to 20 m) and path loss (ranging approximately from 0 to 50 dB) respectively. In comparison, in narrowband indoor systems, the rms value is $19 \sim 49$ ns [78], and increases with the propagation distance [42,47] and with the path loss [47].

3.4. Deterministic Channel Modelling

In addition to channel measurements, preliminary research efforts have been devoted to characterizing the UWB channel based on theoretical approaches [81–84,106]. One important characteristic of UWB propagation is that each path has its own impulse response or frequency transfer function that is frequency dependent [104], which is different from narrowband transmission where the frequency independence assumption is implied [105] and widely adopted. One approach is based on the geometrical theory of diffraction (GTD) which has been used in UWB radar identification [73]. Due to the similarity between the radar objects and the wireless channel obstacles, the approach can be applied to UWB channel modelling with multiple-edge scatterers and the corresponding time-domain resolutions to lower frequencies by including the higher-order multiple diffractions in terms of wave number. All the multiple diffractions are treated together and the total field is decomposed into several leading terms, using the scattering center model. The scattering center model is generalized to include the scattering and diffraction mechanisms, by introducing a frequency dependence factor to the channel gain of each scattered signal component. The multiple diffractions distort the UWB signal waveform significantly and therefore, degrade the signal-to-noise ratio at the correlator output. This suggests that the frequency-dependent effects on the received waveform should be taken into account in the transceiver design, even though the effects are usually negligible in narrowband systems. Another theoretical approach is based on the uniform theory of diffraction (UTD). The received waveform is modelled as a superposition of channel significant rays, taking into

account the effects of the transmitter antenna, multipath propagation, and receiver antenna. For the lth significant ray, the channel is modelled as the tandem of three filters with the transmitter antenna impulse response in the emission direction of the lth ray. The lth channel impulse response takes into account not only the attenuation but also the dispersion due to interaction, and the receiver antenna impulse response in the arrival direction of the lth ray, respectively. The channel for each ray modifies the shape and amplitude of the corresponding impulse in a realistic way. The significant rays and their associated delays between the transmitter and receiver are to be determined by ray tracing. The channel transfer function associated with each ray is determined based on UTD. Based on the delay associated with each ray, the contribution of each ray to the received waveform in the time domain can be obtained from the frequency domain channel function.

In summary, preliminary studies of UWB propagation have confirmed that the well-developed narrowband indoor wireless channel models or parameter values are not appropriate for UWB propagation. Measurement results given in [53,119,122] demonstrate the potential of UWB radio for robust indoor communications at a low transmit power level, which is also confirmed by the measurements reported in [29,113]. However, multiple diffractions are expected to distort UWB signal waveform significantly and therefore, degrade the transmission performance [87]. Extensive field measurements and analysis for various propagation environments, together with more comprehensive theoretical modelling, are required in order to obtain more insights of UWB channel behaviours and, thus, to design the transmitter and receiver to mitigate channel impairments.

4. Receiver Techniques and Transmission Performance

The UWB channel introduces large-scale path loss, shadowing, small-scale fading, and propagation delay dispersion to the transmitted monocycle train. The distorted waveforms arriving at the receiver are further corrupted by multiple access interference, narrowband jamming, and background noise. The function of the receiver is to extract the information bit sequence modulated on the monocycle train from the distorted and corrupted receiving waveforms with a high accuracy. In general, the receiver consists of a detector and a decision device. The detector is different from the demodulator in narrowband systems, due to the fact that UWB transmission is carrier-less. However, many receiver techniques of narrowband systems for forming the decision variable can be directly applied to UWB receivers.

The most common UWB receiver implementations include threshold detectors, autocorrelation receivers, and correlation or rake receivers. The threshold detectors are simple to implement and are suitable for UWB radar systems [3]. An autocorrelation receiver correlates the received waveform with a previously received waveform [16,50,103,104,108], which is similar to the suboptimal differential detector for differential phase shift keying (DPSK) in narrowband systems. It can capture the entire received waveform energy for a slowly varying channel without requiring channel estimation, as the transmitter transmits a pilot (reference) waveform to generate side information about the channel. The receiver suffers from the noise-on-noise effect and 3 dB loss for transmitting the reference waveform [16]. Most research on the receiver focuses on the correlator receiver [9,16,34, 36,85,86,101,116–118,123], which can achieve the optimal performance. As a result, we mainly discuss the correlator receiver in the following.

4.1. Optimum Receiver for AWGN Channel

Consider an AWGN channel in the absence of multiple access interference. The received signal is given by

$$r(t) = x(t) + n(t)$$

where $x(t)$ is the transmitted monocycle train given in Equations (9) and (10), depending on the modulation scheme used, and $n(t)$ is zero-mean white Gaussian noise with two-sided psd of $N_0/2$. Here it is assumed that the effects of the transmitter and receiver antennas on monocycles have been compensated by the pulse generation at the transmitter and receiver respectively. The optimum receiver for the channel is a correlator (i.e. matched filter) receiver. The receiver block diagram is shown in Figure 3, where the receiver locally generated monocycle signal $x_r(t)$ is synchronized with the incoming monocycle train and is given by

$$x_r(t) = \frac{1}{\sqrt{N_s}} \sum_{n=1}^{\infty} \sum_{j=0}^{N_s-1} p_r(t - nT_d - jT_f) \qquad (15)$$

where $p_r(t)$ is a function of j and has unity energy, given by

$$p_r(t) = \begin{cases} \{p[t-(c_t)_j T_c] - p[t-(c_t)_j T_c - \delta]\}/\sqrt{2} & \text{(TH-SS PPM)} \\ (c_d)_j[p(t) - p(t-\delta)]/\sqrt{2} & \text{(DS-SS PPM)} \\ p[t-(c_t)_j T_c] & \text{(TH-SS PAM)} \\ (c_d)_j p(t) & \text{(DS-SS PAM)} \end{cases} \tag{16}$$

At the end of the nth information symbol interval, $t = nT_d$, the decision variable is

$$\begin{aligned} y(nT_d) &= \int_{(n-1)T_d}^{nT_d} r(t)x_r(t)\mathrm{d}t \\ &= \sum_{j=0}^{N_s-1} \int_{(n-1)T_d+jT_f}^{(n-1)T_d+(j+1)T_f} r(t)x_r(t)\mathrm{d}t \\ &= \pm\sqrt{\frac{(1-\rho)N_s E_p}{2}} + N_n \end{aligned}$$

where the "+" sign is for the case that information bit "1" was sent and the "−" sign for the case that "0" was sent, and ρ (equal to 0 for PPM and to -1 for PAM) is the correlation coefficient between the two signals for symbols "1" and "0", respectively, $N_s E_p$ is the bit energy, and $N_n = \int_{(n-1)T_d}^{nT_d} n(t)x_r(t)\mathrm{d}t$ is a Gaussian random variable with zero mean and variance $N_0/2$. Let $\hat{d}_n$ denote the detected nth transmitted information symbol. Then, the maximum likelihood (ML) decision rule is that: if $y(nT_d) \geq 0$, then $\hat{d}_n$ is "1"; otherwise, $\hat{d}_n$ is "0". The probability of bit error, or bit error rate (BER), is given by [48]

$$P_b = Q\left(\frac{\sqrt{(1-\rho)N_s E_p}}{N_0}\right) \tag{17}$$

4.2. Rake Receiver for Frequency-Selective Fading Channel

As discussed in Section 3, the UWB channel introduces frequency-selective fading and the channel can be modelled by a linear tapped-delay-line. Consider a linear tapped-delay-line channel model with the maximum excess delay $\tau_m (\gg T_p)$. For presentation clarity, assume that $T_f \geq T_p + N_t T_c + \delta + \tau_m$ and that $|\tau_l - \tau_{l'}| \geq T_p$ for $l \neq l'$ in PPM so that there is no inter-symbol and inter-monocycle interference. Assume that the channel is time invariant over the duration of a few symbol (bit) intervals. Let $h(t)$ denote the channel impulse response over the time interval. The received signal is then

$$\begin{aligned} r(t) &= x(t) \star h(t) + n(t) \\ &= \sqrt{E_p}\sum_{n=1}^{\infty}\sum_{j=0}^{N_s-1}[p_t(t-nT_d-jT_f) \star h(t)] + n(t) \\ &= n(t) + \sqrt{E_p}\sum_{n=1}^{\infty}\sum_{j=0}^{N_s-1} \begin{cases} q[t-nT_d-jT_f-(c_t)_j T_c - \delta d_n] & \text{(TH-SS PPM)} \\ (c_d)_j q(t-nT_d-jT_f-\delta d_n) & \text{(DS-SS PPM)} \\ q[t-nT_d-jT_f-(c_t)_j T_c]d_n & \text{(TH-SS PAM)} \\ (c_d)_j q(t-nT_d-jT_f)d_n & \text{(DS-SS PAM)} \end{cases} \end{aligned}$$

where the sign "$\star$" denotes convolution, and $q(t) = p(t) \star h(t)$ with a duration $T_q = T_p + \tau_m$. As the channel exhibits frequency-selective fading due to the extremely wideband nature of the transmitted signal, the received signal $r(t)$ is inherent with path diversity. A rake receiver [80] can be used to exploit the diversity by constructively combining the separable monocycles from distinguishable propagation paths for improving transmission performance. Consider a rake receiver with L fingers to collect received signal energy from the L strongest paths having excess delays $\{\tau_l\}|_{l=0}^{L-1}$, where $0 \leq \tau_0 < \tau_1 < \cdots < \tau_{L-1} \leq \tau_m$. Figure 4 shows the receiver block diagram, which consists of L correlators (excluding the decision device shown in Figure 3). The lth correlator (finger), $l = 0, 1, 2, \ldots, L-1$, is to correlate the received signal $r(t)$ with the receiver locally generated reference signal delayed by τ_l, $x_r(t-\tau_l)$. Without loss of generality, consider the detection of the nth information symbol, $n = 1, 2, \ldots$. The output of the lth correlator is

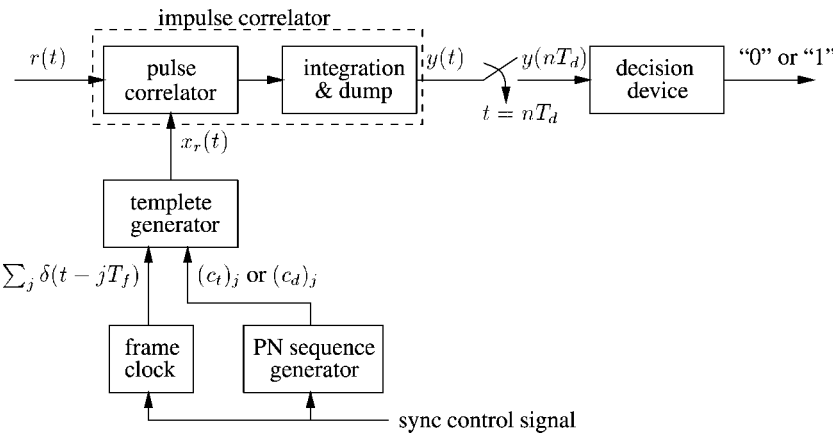

Figure 3. Block diagram of the correlator receiver.

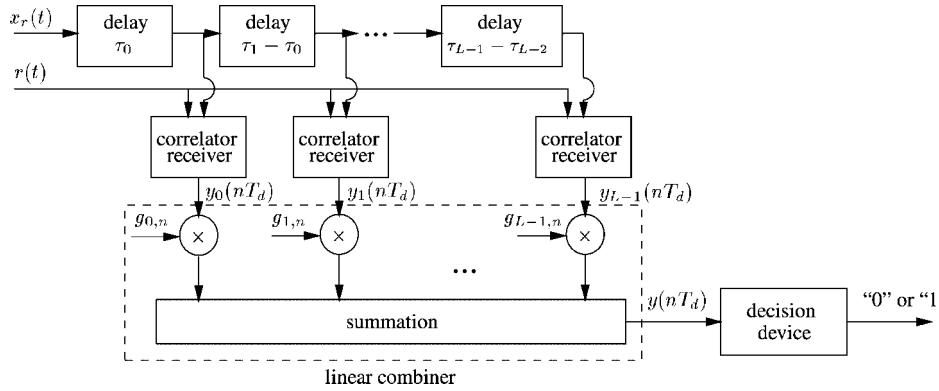

Fig. 4. Block diagram of the rake receiver.

$$y_l(nT_d) = \int_{(n-1)T_d}^{nT_d} r(t)x_r(t-\tau_l)\mathrm{d}t = \pm\sqrt{N_sE_p}\alpha_n(\tau_l) + N_{l,n}$$

where the "+" sign is for symbol "1" and the "−" sign is for symbol "0",

$$\alpha_n(\tau_l) = \left|\int_{(n-1)T_d}^{nT_d} q(t)p_r(t-\tau_l)\mathrm{d}t\right|$$

represents the cross-correlation in magnitude between $q(t)$ and $p_r(t-\tau_l)$, and

$$N_{l,n} = \int_{(n-1)T_d}^{nT_d} n(t)x_r(t-\tau_l)\mathrm{d}t$$

is a zero-mean Gaussian random variable with variance $N_0/2$ and is independent of $n_{l',n'}$ for $l \neq l'$ and/or $n \neq n'$.

The output of the correlators can be linearly combined in different ways to form the decision variable $y(nT_d)$ [80], among which the maximal ratio combining approach, with $g_{l,n} = \sqrt{N_sE_p}\alpha_n(\tau_l)$, provides the optimal performance [6]. The performance is achieved at the cost that the channel information $h(t)$ is required at the receiver. The output of the maximum ratio combiner is given by

$$\begin{aligned} y(nT_d) &= \sum_{l=0}^{L-1} \sqrt{N_sE_p}\alpha_n(\tau_l)y_l(nT_d) \\ &= \pm N_sE_p \sum_{l=0}^{L-1} \alpha_n^2(\tau_l) + N_n \end{aligned} \tag{18}$$

where $N_n = \sqrt{N_sE_p}\sum_{l=0}^{L-1}\alpha_n(\tau_l)N_{l,n}$ follows the Gaussian distribution with zero mean and variance equal to $[N_sE_p\sum_{l=0}^{L-1}\alpha_n^2(\tau_l)](N_0/2)$. Derivation of the transmission bit error probability in general is very complex as the decision variables for symbol "1" and symbol "0" are not independent. For PPM, under the simplified assumptions that $\alpha_n(\tau) = 0$ for $\tau \leq T_p$ or $\tau \geq T_q$, and that $\int_{-\infty}^{\infty} p_r(t)p_r(t-\tau)\mathrm{d}t = 0$ for

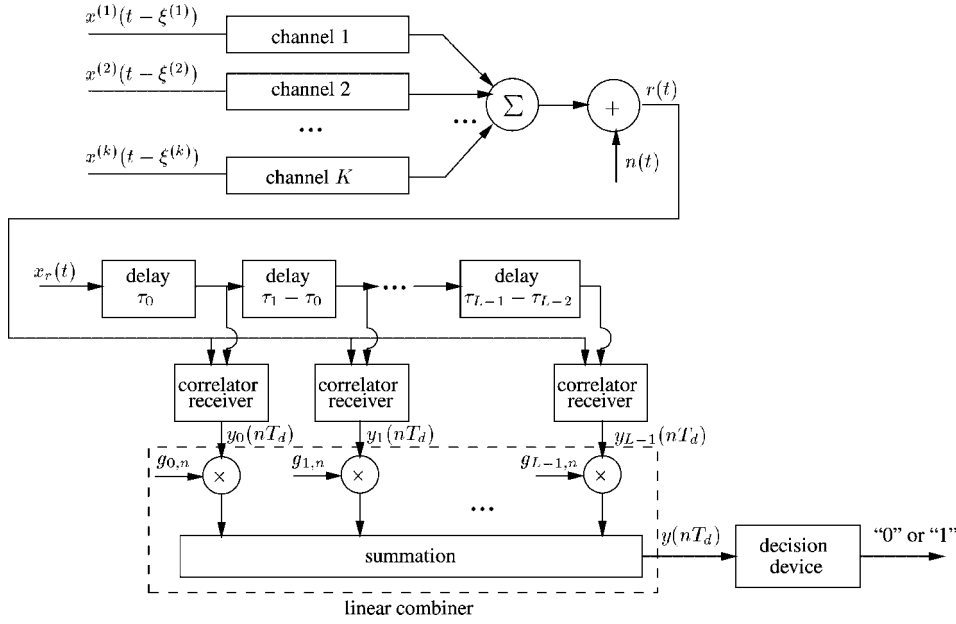

Fig. 5. Block diagram of the multiple-access transmission system.

$|\tau| > T_p$, the probability of bit error can be derived as [16]

$$P_b = Q\left(\frac{\sqrt{N_s E_p \sum_{l=0}^{L-1} \alpha_n^2(\tau_l)}}{N_0}\right) \tag{19}$$

Note that Eq. (19) includes Eq. (17) as a special case for PPM with $\rho = 0$, $L = 1$, and $\alpha_n(\tau_0) = 1$.

4.3. Detection in the Presence of Multiple Access Interference

Consider a multiple-access system with K active users. Let superscript (k) indicate the functions and variables associated with user k. The transmitting signals are $\{x^{(k)}(t^{(k)})\}|_{k=1}^{K}$, where the clocks of the transmitters are not synchronized and $t^{(k)}$ denotes the kth user transmitter clock time. The composite received signal in a frequency-selective fading environment is

$$r(t) = \sum_{k=1}^{K} x^{(k)}(t-\xi^{(k)}) \star h^{(k)}(t-\xi^{(k)}) + n(t) \tag{20}$$

where t is the receiver clock time, $\xi^{(k)}$ is the difference between the receiver clock and the kth transmitter clock (i.e., $\xi^{(k)} = t^{(k)} - t$), and $h^{(k)}(t^{(k)})$ is the channel impulse response experienced by the kth transmitted signal. Without loss of generality, consider the detection of the first $(k = 1)$ user's signal using the rake receiver with maximal ratio combining and assume that the receiver clock is synchronized with the transmitter clock (i.e., $\xi^{(1)} = 0$). The system block diagram is shown in Figure 5. The decision variable is given by

$$y(nT_d) = \pm N_s E_p^{(1)} \sum_{l=0}^{L-1} \left[\alpha_n^{(1)}(\tau_l)\right]^2 + N_n + I_n \tag{21}$$

which is the same as Equation (18) except the third term I_n representing the multiple access interference (MAI). The MAI is given by

$$I_n = \sum_{k=2}^{K} \sqrt{E_p^{(k)} E_P^{(1)}} \sum_{l=0}^{L-1} \alpha_n^{(1)}(\tau_l) \int_{(n-1)T_d}^{nT_d} \times \left\{ \sum_{n_1=1}^{\infty} \sum_{j_1=0}^{N_s-1} \left[p_t^{(k)}(t-\xi^{(k)} - n_1 T_d - j_1 T_f) \star h^{(k)}(t-\xi^{(k)})\right] \right\} \times \left[\sum_{n_2=1}^{\infty} \sum_{j_2=0}^{N_s-1} p_r^{(1)}(t - n_2 T_d - j_2 T_f)\right] \mathrm{d}t$$

Statistics of the MAI are difficult to compute in general due to the large number of variables involved and the correlation among the variables. As a result, the probability of bit error versus K (the number of

users) is obtained via computer simulation and reported in [101] for TH-SS PPM for flat fading channel and exponentially decaying frequency-selective fading channels.

In TH-SS PPM, with a sufficiently large ratio $N_s T_c / T_f$ and properly designed TH sequences, the MAI in an AWGN channel can be approximated by a Gaussian random process [93]. Under the assumption of Gaussian distributed interference, the performance in terms of achievable transmission rate and multiple-access capability is estimated and presented in [116].

The rake receiver shown in Figure 5 is the conventional signal-user detector. For PPM, when the received monocycle positions between any two users do not overlap, the rake receiver with a large number of taps is approximately optimum. In general, MAI is not Gaussian and therefore, the receiver is non-optimal for all the four UWB schemes.

The optimum receiver in the presence of MAI is one that performs maximum-likelihood sequence detection jointly across all users' sequences [25,110]. Many multi-user detection techniques [110] developed for narrowband systems can be applied to multiple access UWB systems to combat MAI and to improve the system performance, at the cost of much more complex receiver design [68,76,123].

4.4. Challenges in Receiver Design

One advantage of UWB systems is the availability of low-cost transceivers, as mentioned in Section I. However, current embodiments of UWB receivers sacrifice performance for low-complexity operation. A large discrepancy in performance exists between the implementations and the theoretically optimal receiver [16]. Extensive R&D activities are required to improve the transmission performance and, at the same time, to reduce the receiver complexity. Issues that should be addressed include the following:

(1) In the above study of correlator receivers, it is assumed that the receiver locally generated monocycles are synchronized with the target input signals. Indeed, high synchronization accuracy is required, because UWB system performance is very sensitive to the timing jitter due to the extreme short monocycle width [71]. Rapid and accurate time synchronization techniques need to be investigated and developed;
(2) In addition to amplitude fading and propagation delay spread, the UWB channel introduces monocycle waveform distortion, due to the fact that each propagation path experiences frequency-dependent fading. The distortion results in receiver performance degradation [84]. The distortion should be characterized and the transceiver should be designed to compensate for the channel effect;
(3) Further research is necessary to compare the four UWB schemes given in Equations (9) and (10) and to investigate higher-order modulation for UWB transmission in terms of the tradeoff between the implementation cost and performance (such as transmission accuracy and system capacity or throughput over a multipath propagation channel in the presence of multiple access interference);
(4) Channel estimation (in terms of amplitude attenuation and propagation delay) is necessary for the operation of the rake receiver and multiuser detection. Errors in the channel estimation can significantly degrade the transmission performance, especially when the number of active users is relatively large [70]. Furthermore, the application of multiuser detection techniques to UWB receivers deserves more attention. A good compromise between performance improvement and receiver complexity should be reached for a practical UWB transmission system.

5. Resource Management for QoS Provisioning

In the past few years, first-generation multimedia capabilities have become available on portable PCs, reflecting the increasing mainstream role of multimedia in computer applications. As multimedia features continue their inevitable migration to portable devices such as laptop PCs, personal digital assistants (PDAs), and personal information assistants (PIAs), wireless extensions to wireline broadband networks will have to support an integrated mixture of multimedia traffic (such as voice, high-rate data, and streaming video) with guaranteed quality of service (QoS). With the potential high transmission rates, UWB systems are expected to provide multimedia services in a wide set of applications, from wireless personal area networks (PAN) to wireless *ad hoc* networks.

The multimedia services can be of any nature, including the constant-rate traffic for uncompressed voice and video, variable-rate traffic for compressed voice and video, and available-rate traffic for data.

The information sources can exhibit highly bursty traffic rates. Packetized transmission over UWB links makes it possible to achieve a high statistical multiplexing gain. Depending on the application, the QoS requirements of each connection can be specified by physical layer parameters such as BER, link layer parameters such as packet loss rate, packet delay and delay jitter, and network layer parameters such as new call-blocking probability and handoff call-dropping probability. As a result, effective and efficient resource and mobility management at both link and network layers are essential to UWB multimedia services to achieve service quality satisfaction, in addition to transmission technologies at the physical layer.

Up to now, most of the R&D efforts on UWB systems have been devoted to the transmission issues at the physical layer. Resource and mobility management at the link and network layers is still embryonic, but its important role has started to be recognized [2,23,35,62,77,100,112]. As far as the resource and mobility management is concerned, there are many open issues. Special network mechanisms are needed in order to efficiently accommodate a large variety of mobile users with different service rates in a band width-on-demand fair-sharing manner. A defining characteristic of wireless mobile networks is that the point of attachment to the network changes. The expected provision of flexible high-rate services in the mobile environment leads to increased complexity in resource control and management because of the variable and unpredictable bandwidth requirements of multimedia applications. Heterogeneity is another dimension induced by different behaviours of the coexisting networks.

5.1. Network Architecture

In recent years, the proliferation and universal adoption of the Internet as the information transport platform have escalated it as the key wireline network for supporting fixed terminals. As a result, the next-generation wireless networks are evolving toward a versatile IP (Internet Protocol) based network that can provide various real-time multimedia services to mobile users [74]. Various mechanisms have been proposed for QoS provisioning in the IP networks, among which the integrated services (IntServ) approach and the differentiated services (DiffServ) approach [4] are the two main architectures. The IntServ approach uses the Resource Reservation Protocol (RSVP) to explicitly signal and dynamically allocate resources at each intermediate node along the path for each traffic flow. In this model, every change in a mobile host[5] (MH) attachment point requires new RSVP signalling to reserve resources along the new path. Also, the heavy signalling overhead reduces the utilization efficiency of the wireless bandwidth. On the other hand, the 'DiffServ' approach uses a much coarser differentiation model to obviate the above disadvantages, where packets are classified into a small number of service classes at the network edge. The packets of each class are marked and traffic conditioned by the edge router, according to the resource commitment negotiated in the service level agreement (SLA). In each core router, QoS for different classes is differentiated by different *per-hop behaviours*. Resource allocation is performed by the *bandwidth broker* in a centralized manner, without dynamic resource reservation signalling and reservation status maintaining in the core routers. Figure 6 shows a generic hybrid UWB wireless/IP network architecture based on the DiffServ approach, where the wireless segment includes both infrastructure-based pico-cellular subnets and infrastructureless ad hoc subnets. Some of the pico-cellular subnets are based on UWB technologies, depending on the system design performance criteria and application environment. In the ad hoc subnets, each MH assumes a double role of terminal and router; an MH is connected to the wireline domain probably via a multiple-hop link. An important design strategy for the network architecture is to have a generic IP network layer which is compatible with the network layer of the Internet and other narrowband wireless systems, and to design a link layer which adapts to and utilizes the particular properties of the physical-layer UWB transmission. How to solve the backward compatibility is a key issue and needs further research.

5.2. Domain-Based Call Admission Control

In the network architecture, all the registration domains are DiffServ administrative domains in which all the routers are DiffServ IP routers. The gateway and base stations are edge routers, and they are connected through core routers. The gateway is the interface connecting to the DiffServ Internet backbone, where an SLA is negotiated to specify the resources allocated by the Internet service provider

[5]Here, the terms *mobile user* and *mobile host* are used interchangeably, as these terms are being used quite freely in the literature.

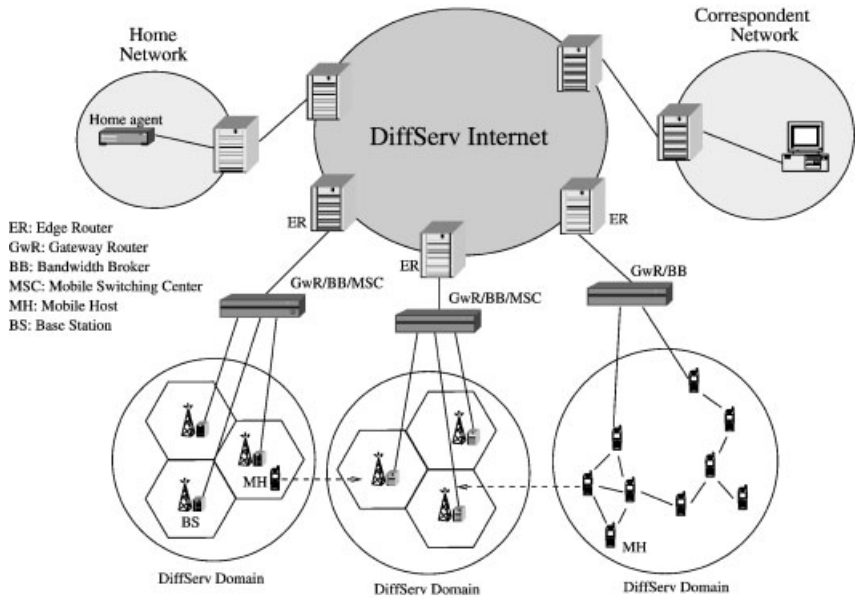

Fig. 6. A conceptual model of DiffServ registration-domain-based UWB wireless network architecture.

to serve the aggregate traffic flowing from/into the gateway. The gateway conditions the aggregate traffic for each class according to the SLA resource commitments. All the MHs in the same registration domain are connected to the same gateway router. All DiffServ routers use three separate queues to provide the premium service, the assured service and the best-effort service respectively [12]. The three buffers are served under priority scheduling or weighted fair queue (WFQ) scheduling. The traffic classes provided by the UWB wireless subnets can be mapped to these three DiffServ classes. For example, the conversational class and the streaming class can be mapped to the premium service and the assured service, respectively, while the interactive class or the background traffic can be mapped to the best effort class. The advanced two-tier resource management (ATTRM) model [14] can be applied for efficient resource allocation in the DiffServ network, where the multi-protocol label switching (MPLS) technique is used to establish a path-oriented environment in a DiffServ domain. By proper boundary SLA arrangements, per-flow explicit admission control and routing, the bandwidth broker can configure the core routers accurately. End-to-end QoS support is achieved through the concatenation of QoS support in each and every domain along the connection path. The domain under consideration has a general architecture, and can deploy IP based micromobility protocols (such as Cellular IP [7], MCIP [69] and HAWAII [88]) which complement the Mobile IP by providing fast, seamless and local handoff control.

An important issue to maintain satisfactory service quality is call admission control (CAC) which limits the number of concurrent users. For each connection request, the CAC routine is to check whether there are sufficient resources available to serve the new call and the rest on-going calls with guaranteed QoS. If the answer is yes, the new call is admitted; otherwise, rejected. The objective of CAC is to simultaneously guarantee QoS and achieve high resource utilization. A significant amount of research on CAC has been done for packet-switching wireline networks [96], and more recently for circuit-switching wireless communications [30,49,120]. In the research for wireline networks, QoS of interest is mainly at the network layer as there is no handoff in the network and wireline links provide reliable transmission. Due to its complex nature, most previous works on CAC for wireless mobile systems are limited to circuit-switching voice services, and the performance criteria are specified at the network and physical layers, under the assumptions that the interval between call arrivals, cell residence time and call duration are independently and exponentially distributed [15]. For packet-switching UWB systems, CAC needs to ensure QoS provisioning at all the three (network, link, and physical) layers. The capacity calculation in the previous work for continuous transmission [100] needs to be extended to discrete packetized transmission,

taking into account the packet data traffic characteristics. Moreover, performance of a CAC algorithm depends on user mobility. Even though simplified assumption of Poisson new and handoff call arrivals and exponential channel holding time could facilitate initial investigation of CAC, more practical user traffic models and user mobility models should be developed for CAC in the UWB environment.

One approach to represent the amount of resources required by each traffic flow from a mobile or fixed host is to use the *effective bandwidth* concept [13,26,27,43,55,58,61]. Effective bandwidth is defined as the minimum link capacity required to satisfy the physical-layer and link-layer QoS requirements, taking into account the packet flow statistics, the user mobility pattern, and possibly the statistical multiplexing among all the users sharing the common resources. In this way, the call-level QoS provisioning at the network layer can be decoupled from that at the physical and link layers [67,126]. The resource commitments specified in the SLA can then be represented in terms of number of calls of each class is allowed in the registration domain. As a result, the admission control procedure can be straightforward: whenever a new MH requests admission to a registration domain, the bandwidth broker determines whether to admit or reject the new call, based on the number of the calls currently in service and the SLA allocation for the service class to which the new call subscribes. The new call has to be dropped if all the SLA allocation has been occupied. This procedure requires very simple communications between the edge router (the base station) and the bandwidth broker (in the gateway router) and can be executed instantly. Furthermore, once an MH is admitted to a registration domain, it can hand off to other cells within the domain without the involvement of further call admission control in the bandwidth broker.

5.3. Resource Allocation and Medium Access Control

In the network architecture, as the layers of the protocol stack cannot operate independently of each other, vertical coupling between layers is critical to high resource utilization and QoS provisioning. In this vein, resource allocation at both link and network layers should be *adaptive* to network conditions (i.e. 'network-aware') and specific user application characteristics (i.e. 'application-aware'). For each mobile connection, the network conditions include UWB link quality (such as fading status, propagation path loss, multiple access interference, narrowband jamming, and noise disturbance), power constraint in UWB transmission, available bandwidth in each node along the connection path, and user mobility information. User application characteristics include service priority/class, transmission delay and delay jitter requirements, required transmission accuracy (in terms of BER and packet loss rate), and peak/average transmission rates. For example, the quality of real-time applications such as video depends very heavily on packet loss and/or jitter due to fading and handoff, whereas application requirements are met for best-effort (data) traffic as long as the network provides some reasonable throughput. Therefore, real-time applications that require more stringent guarantees are more susceptible to such QoS fluctuations. Also, applications that consist of many components (e.g. Web browsing) with temporal dependency among these components need to have certain guarantees which are a combination of non-real-time and real-time requirements. In order to balance the QoS rendered to individual users and the efficient use of the available network resources, adaptive mobility and resource management should allow a tradeoff between different objectives, for example, taking into account the cost of a call dropping and the cost of using link capacity.

Medium access control (MAC) is a link-layer resource management function for QoS provisioning at both the physical layer and link layer. Given the statistics of the UWB channel, spread spectrum and modulation scheme, rake receiver structure and diversity combining technique, the required BER can be mapped one-to-one to the required ratio of signal energy per bit to interference plus noise density at the receiver. The BER requirement can then be satisfied by proper transmit power allocation (probably via power control for a given estimate of the propagation path loss, MAI and background noise) and error control such as using automatic retransmission request (ARQ) techniques. The packet loss rate, delay, and delay jitter requirements can be guaranteed by proper packet scheduling at the link layer [54]. In particular, characteristics of UWB physical layer transmission should be exploited in the link-layer resource allocation. These include the following:

(1) UWB transmission has the flexibility in reconfiguring data rate and power, due to the availability of a number of transmission parameters as given in Section 2, which can be tuned to better match different signalling/information data transmission

requirements on a per-packet and/or per-link basis. The flexibility facilitates joint power and rate allocation at the link layer for maximal resource utilization under the QoS constraint [99];

(2) UWB transmission offers the potential of accurate user location. The location information can be used for transmission synchronization, power and rate allocation, and for traffic routing in an *ad hoc* environment. QoS provision in ad hoc networks involves QoS support in MAC protocols [98] and QoS routing [57]. QoS support in wireless *ad hoc* networks is a new but growing area of research [10]. The availability of accurate MH position in UWB systems can greatly simplify traffic routing and improve throughput in ad hoc systems. In addition, UWB transmission requires the synchronization of each transmitting-receiving pair (communicating through a link), but works efficiently even though different links in the network are asynchronous. This feature is particularly suitable for the ad hoc subnet, where the absence of a fixed infrastructure implies a highly complex synchronization of all the network terminals;

(3) UWB systems will coexist with other wireless systems in the same coverage area. Interference from/to other systems will limit the UWB throughput and should be monitored in the link layer resource allocation;

(4) Handoff from/to other wireless systems (in the same or different coverage areas) will occur to provide ubiquitous coverage. In such a heterogeneous networking environment, a distributed MAC mechanism is a preferred choice to a centralized one, even though the distributed solution introduces complexity in the resource allocation. Distributed MAC that allows flexible, fast, and efficient resource sharing for QoS satisfaction is a desired solution [18,23]. The inherent spread spectrum in UWB transmission can facilitate multiple access by proper PN code design and CAC; furthermore, time-division multiple access can be implemented for packetized transmission, which adds more design choices and control flexibility in the link-layer resource allocation [54].

Physical layer state information needs to be identified and defined, and techniques to estimate the state information/parameters need be developed. A flexible resource allocation scheme for medium access control and for packet transmission scheduling based on the physical layer state information is required to efficiently accommodate multimedia traffic flows in UWB transmission.

In summary, the perspective of today's information society calls for a multiplicity of devices, including IP-enabled home appliances, personal computers, sensors, and so on, to be globally connected. To cope with these complex connectivity requirements, current mobile and wireless systems and architectural concepts must evolve. This evolution has far reaching implications, with users and information devices capable of roaming across a variety of heterogeneous network and service environments, operating in various frequency bands, and employing adapted air interfaces for optimal use of radio resources. In this context, the key issue is how to achieve cooperation and seamless interworking at service and control planes of multiple pervasive-access wireless technologies (including cellular, personal area, local area, fixed wireless, ad hoc wireless, etc.) over a common IP-based platform, supporting a variety of service requirements. Among these, seamless interworking between UWB wireless systems and the Internet is a key research area in order to unleash the full potential of UWB applications and services. Further research on network architectures, mobility management protocols, and resource allocation algorithms are required for providing multimedia services with QoS support using UWB technologies.

6. Conclusions

UWB transmission systems have advantages including high data rate, robust to multipath fading, potential low-cost transceiver implementations, accurate mobile user location, and coexistence with narrowband wireless systems. However, development of UWB technology to live up to its full potential still poses significant technical challenges. These include accurate channel characterization, transceiver design with high performance at low implementation complexity, narrowband interference suppression and, in particular, resource allocation at the link and network layers to support multimedia services with QoS provisioning.

This paper provides an overview of the fundamentals of UWB wireless high-rate short-range communications. It studies the details of impulse radio transmission techniques, channel models and statistics, and reception techniques. It also discusses some important issues in resource allocation at the link and network layers for multimedia services with QoS support, such as the UWB/IP interworking architecture, call admission control, and medium access

control. The previous research results are presented, and further research topics are identified.

Acknowledgement

Weihua Zhuang, Xuemin (Sherman) Shen wish to thank their Ph.D. students (J. Cai, Y. Cheng, and L. Xu) at the Centre for Wireless Communications, University of Waterloo, for collecting previous publications on UWB which helped this research.

References

1. Adams JC, Gregorwich W, Capots L, Liccardo D. Ultra-wideband for navigation and communications. *Proceedings of IEEE Aerospace Conference* 2001; **2**: 785–791.
2. Baldi P, Nardis LD, Benedetto MD. Modeling and optimization of UWB communication networks through a flexible cost function. *IEEE Journal on Selected Areas in Communications* 2002; **20**(9): 1733–1744.
3. Bennett CL, Ross GF. Time-domain electromagnetics and its applications. *Proceedings of the IEEE* 1978; **66**(3): 299–318.
4. Blake S, Black D, Carlson M, Davies E, Wang Z, Weiss W. *An Architecture for Differentiated Services*, IETF RFC 2475, Dec. 1998.
5. Blefari-Melazzi N, Benedetto MGD, Gerla M, Luediger H, Win MZ, Withington P. Guest editorial ultra-wideband radio in multi-access wireless communication. *IEEE Journal on Selected Areas in Communications* 2002; **20**(9): 1609–1611.
6. Brennan DG. Linear diversity combining techniques. *Proceedings of the IRE* 1959; **47**: 1075–1102.
7. Campbell AT, Gomez J, Kim S, Valko AG, Wan C, Turanyi ZR. Design, implementation and evaluation of Cellular IP. *IEEE Personal Communications* 2000; **7**(4): 42–49.
8. Cassioli D, Win MZ, Molisch AF. The ultra-wide bandwidth indoor channel: from statistical model to simulations. *IEEE Journal on Selected Areas in Communications* 2002; **20**(6): 1247–1257.
9. Cassioli D, *et al.* Performance of low-complexity rake reception in a realistic UWB channel. *Proceedings of IEEE ICC* 2002; 763–767.
10. Chakrabarti S, Mishra A. QoS issues in ad hoc wireless networks. *IEEE Communications Magagine* 2001; **39**(2): 142–148.
11. Chen X, Kiaei S. Monocycle shapes for ultra-wideband system. *Proceedings of IEEE ISCAS* 2002; **1**: I-597–I-600.
12. Cheng Y, Zhuang W. Optimal buffer partitioning for multiclass Markovian traffic sources. *Proceedings of IEEE Globecom* 2001; 1852–1856.
13. Cheng Y, Zhuang W. Effective bandwidth of multiclass Markovian traffic sources and admission control with dynamic buffer partitioning. *IEEE Transactions on Communications* (to appear), also in *Proceedings of IEEE Globecom* 2002; 2548–2552.
14. Cheng Y, Zhuang W. Efficient resource allocation over MPLS differentiated services networks. *Proceedings of 3Gwireless* 2002; 749–754.
15. Leong CW, Zhuang W. Call admission control for wireless personal communications. *Computer Communications* 2003; **26**(6): 522–541.
16. Choi JD, Stark WE. Performance of ultra-wideband communications with suboptimal receivers in multipath channels. *IEEE Journal on Selected Areas in Communications* 2002; **20**(9): 1754–1766.
17. Conroy JT, LoCicero JL, Ucci DR. Communication techniques using monopulse waveforms. *Proceedings of MILCOM* 1999; **2**: 1181–1185.
18. Corson MS, Loroia R, O'Neill A, Park V, Tsirtsis G. A new paradigm for IP-based cellular networks. *IEEE IT Proceedings* Nov/Dec. 2001; 20–29.
19. Cramer RJ, Scholtz RA, Win MZ. Evaluation of an ultra-wideband propagation channel. *IEEE Transactions of Antennas Propagations* 2002; **50**(5): 561–570.
20. Cramer RJ. An evaluation of ultra-wideband propagation channels. PhD Dissertation, Univ. of Southern California, Dec. 2000.
21. Cramer RJ, Scholtz RA, Win MZ. On the analysis of UWB communication channels. *Proceedings of IEEE MILCOM* 1999; 1191–1195.
22. Cramer RJ, Scholtz RA, Win MZ. Spatio-temporal diversity in ultra-wideband radio. *Proceedings of IEEE WCNC* 1999; **2**: 888–892.
23. Cuomo F, Martello C, Baiocchi A, Capriotti F. Radio resource sharing for ad hoc networking with UWB. *IEEE Journal on Selected Areas in Communications* 2002; **20**(9): 1722–1732.
24. Discrete Time Communications. ''New'' ultra-wideband technology. White Paper, Oct. 2002.
25. Duel-Hallen A, Holtzman J, Zvonar Z. Multiuser detection for CDMA systems. *IEEE Personal Communications* 1995; **2**(2): 46–58.
26. Elwalid AI, Mitra. Effective bandwidth of general Markovian traffic sources and admission control of high speed networks. *IEEE/ACM Transactions Networking* 1993; **1**(3): 329–343.
27. Evans JS, Everitt D. Effective bandwidth-based admission control for multiservice CDMA cellular networks. *IEEE Transactions on Vehicular Technology* 1999; **48**(1): 36–46.
28. Eshima K, Hase Y, Oomori S, Takahashi F, Kohno R. *M*-ary UWB system using Walsh codes. *Proceedings of IEEE Conference Ultra-Wideband Systems and Technologiesogies* 2002: 37–40.
29. Estes DRJ, Welch TB, Sarkady AA, Whitesel H. Shipboard radio frequency propagation measurements for wireless networks. *Proceedings of IEEE MILCOM* 2001; **1**: 247–251.
30. Fang Y, Zhang Y. Call admission control schemes and performance analysis in wireless mobile networks. *IEEE Transactions Vehicle Technologies* 2002: **51**(2): 371–382.
31. Farr EG, Bowen LH. Recent progresses in impulse radiating antennas. *Proceedings of IEEE Conference Ultra-Wideband Systems and Technologies*, Baltimore, USA 2002; 337–340.
32. First Report and Order in the Matter of Revision of Part 15 of the Commission's Rules Regarding Ultra-Wideband Transmission Systems. ET Docket 98–153, Federal Communications Commission, FCC 02–48, April 22, 2002.
33. Fleming R, Kushner C, Roberts G, Nandiwada. Rapid acquisition for ultra-wideband localizers. *Proceedings of IEEE Conference Ultra-Wideband Systems and Technologiesogies* 2002: 245–250.
34. Foerster JR. The performance of a direct sequence spread'ultra wideband system in the presence of multipath, narrowband interference, and multiuser interference. *Proceedings of IEEE Conference Ultra-Wideband Systems and Technologiesogies* 2002: 87–92.
35. Foerster J, Green E, Somayazalu S, Leeper D. Ultra-wideband technologiesogy for short- or medium-range wireless communications. *Intel Technologiesogy Journal* 2001; **Q2**: 1–11.
36. Foerster JR. The effect of multipath interference on the performance of UWB systems in an indoor wireless channel. *Proceedings of IEEE VTC* Spring 2001: 1176–1180.
37. Fontana RJ. Recent applications of ultra wideband radar and communications systems. *Ultra-Wideband, Short-Pulse Electromagnetics*, Kluwer Academic/Plenum Publishers, 2000.

38. Fontana RJ, Ameti A, Richley E, Beard L, Guy D. Recent advances in ultra wideband communications systems. *Proceedings IEEE Conference Ultra-Wideband Systems and Technologies* 2002; 129–133.
39. Fontana RJ, Richley EA, Marzullo AJ, Beard LC, Mulloy RWT, Knight EJ. An ultra-wideband radar for micro air vehicle applications. *Proceedings IEEE Conference Ultra-Wideband Systems and Technologies* 2002; 187–192.
40. Fontana RJ, Gunderson SJ. Ultra-wideband precision asset location system. *Proceedings of IEEE Conference Ultra-Wideband Systems and Technologies* 2002; 147–150.
41. Fullerton L. UWB waveforms and coding for communications and radar. *Proceedings IEEE Telesystems Conference* 1991; 139–141.
42. Greenstein LJ. A new path-gain/delay-spread propagation model for digital cellular channels. *IEEE Transactions on Vehicular Technology* 1997; **46**(2): 477–485.
43. Guerin R, Ahmadi H, Naghshineh M. Equivalent capacity and its application to bandwidth allocation in high-speed networks. *IEEE Journal on Selected Areas in Communications* 1991; **9**(7): 968–981.
44. Hamalainen M, Hovinen V, Tesi R, Iinatti JHJ, Latva-aho M. On the UWB system coexistence with GSM900, UMTS/WCDMA, and GPS. *IEEE Journal on Selected Areas in Communications* 2002; **20**(9): 1712–1721.
45. Hamalainen M, Tesi R, Iinatti J. On the UWB system performance studies in AWGN channel with interference in UWTS band. *Proceedings of IEEE Conference on Ultra-Wideband Systems and Technologies* 2002; 321–325.
46. Han J, Nguyen C. A new ultra-wideband, ultra-short monocycle pulse generator with reduced ringing. *IEEE Microwave and Wireless Component Letter* 2002; **12**(6): 206–208.
47. Hashemin H. The indoor radio propagation channel. *Proceedings of IEEE* 1993; **81**(7): 943–968.
48. Haykin S. *Communication Systems*, 4th edn. John Wiley & Sons: New York, 2001.
49. HO C-J, Copeland JA, Lea C-T, Stuber GL. On call admission control in DS/CDMA cellular networks. *IEEE Transactions on Vehicular Technology* 2001; **50**(1): 59–66.
50. Hoctor RT, Tomlinson TW. Delay-hopped transmitted-reference RF communications. *Proceedings of IEEE Conference Ultra-Wideband Systems and Technologies* 2002; 265–270.
51. Hogbom JA. Aperture synthesis with a non-regular distribution og interferometer baselines. *Astronmy And Astrophysis Supplementary Series* 1974; **15**.
52. Holzheimer T. The low dispersion coaxial cavity as an ultra wideband antenna. *Proceedings of IEEE Conference on Ultra-Wideband Systems and Technologies* 2002; 333–336.
53. Hovinen V, Hamalainen M, Patsi T. Ultra wideband indoor radio channel models: preliminary results. *Proceedings of IEEE Conference Ultra-Wideband Systems and Technologies* 2002: 75–79.
54. Huang V, Zhuang W. QoS-oriented access control for 4G mobile multimedia CDMA communications. *IEEE Communication Magazine* 2002; **40**(3): 118–125.
55. Hui JY. Resource allocation for broadband networks. *IEEE Journal on Selected Areas in Communications* 1988; **6**(9): 1598–1608.
56. Hussain MGM. Principles of space-time array processing for ultrawide-band impulse radar and radio communications. *IEEE Transactions on Vehicular Technology* 2002; **51**(3): 393–403.
57. Iwata A, Chiang C, Pei G, Gerla M, Chen T. Scalable routing strategies for ad hoc wireless networks. *IEEE Journal on Selected Areas in Communications* 1999; **17**(8): 1369–1379.
58. Kelly FP. Effective bandwidths at multi-class queues. *Queueing Systems* 1991; **9**(1): 5–16.
59. Kelly D, Reinhardt S, Stanley R, Einhorn M. PulsON second generation timing chip: enabling UWB through precise timing. *Proceedings of IEEE Conference Ultra-Wideband Systems and Technologies* 2002; 117–121.
60. Kenington PB, Gillard SJ, New AE. An ultra-broadband power amplifier using dynamically controlled linearisation. *IEEE MTT-S Digest* 1999; 355–357.
61. Kesidis G, Walrand J, Chang C. Effective bandwidths for multiclass Markov fluids and other ATM sources. *IEEE/ACM Transactions on Networking* 1993; **1**(4): 424–428.
62. Kolenchery S, Townsend JK, Freebersyser JA. A novel impulse radio network for tactical military wireless communications. *Proceedings of IEEE MILCOM* 1998; **1**: 59–65.
63. Kouyoumjian R, Pathack PH. A uniform geometrical theory of diffraction for an edge of perfectly conducting surface. *Proceedings of the IEEE* 1974; **62**(11): 1448–1461.
64. Larrick JF, Jr, Fontana RJ. Waveform adaptive ultra-wideband transmitter. U.S. Patent 6,026,125, Feb. 2000.
65. Lee JS, Nguyen C. Novel low-cost ultra-wideband, ultra-short-pulse transmitter with MESFET impulse-shaping circuitry for reduced distortion and improved pulse repetition rate. *IEEE Microwave and Wireless Component Letters*. 2001; **11**(5): 208–210.
66. Leeper D. A long-term view of short-range wireless. *IEEE Computer* 2001; **34**(6): 39–44.
67. Levine DA, Akyildiz AF, Naghshineh M. A resource estimation and call admission algorithm for wireless multimedia networks using the shadow cluster concept. *IEEE/ACM Transactions on Networking* 1997; **5**(1): 1–12.
68. Li Q, Rusch LA. Multiuser detection for DS-CDMA UWB in the home environment. *Journal on Selected Areas in Communications* 2002; **20**(9): 1701–1711.
69. Liu X. Inter-Cluster Soft Handoff in 3G/IP Interworking. MASc Thesis, University of Waterloo, 2002.
70. Lottici V, D'Andrea A, Mengali U. Channel estimation for ultra-wideband communications. *IEEE Journal on Selected Areas in Communications* 2002; **20**(9): 1638–1645.
71. Lovelace WM, Townsend JK. The effects of timing jitter and tracking on the performance of impulse radio. *IEEE Journal on Selected Areas in Communications* 2002; **20**(9): 1646–1651.
72. Loyka S, Kouki A. Using two ray multipath model for microwave link budget analysis. *IEEE Antennas and Propagation* 2001; **43**(5): 31–36.
73. Luebbers RJ, Foose WA, Reyner G. Comparison of GTD propagation model wide-band path loss simulation with measurements. *IEEE Transactions on Antennas Propagation* 1988; **37**(4): 499–505.
74. Mark JW, Zhuang W. *Wireless Communications and Networking*. Prentice-Hall: Upper Saddle River, NJ. 2003.
75. Mitchell T. Broad is the way. *IEE Review* Jan. 2001; 35–39.
76. Muqaibel A, Woerner B, Riad S. Application of multi-user detection techniques to impulse radio time hopping multiple access systems. *Proceedings of IEEE Conference Ultra-Wideband Systems and Technologies* 2002; 169–173.
77. Nardis LD, Baldi P, Benedetto MD. UWB ad-hoc networks. *Proceedings of IEEE Conference Ultra Wideband Systems and Technologies* 2002; 219–223.
78. Pahlavan K, Levesque AH. *Wireless Information Networks*. John Wiley & Sons: New York, 1995.
79. *Proceedings of 2002 IEEE Conference on Ultra-Wideband Systems and Technologies*, Baltimore, May 2002.
80. Proakis JG. *Digital Communications*. McGraw-Hill: New York, 1995.
81. Qiu RC, Lu I-T. A novel high-resolution algorithm for ray path resolving and wireless channel modelling. *Proceedings of IEEE Princeton Sarnoff Symposium* 1995; **0**: 59–63.
82. Qiu RC. A theoretical study of the ultra-wideband wireless propagation channel based on the scattering centers. *Proceedings of IEEE VTC* 1998; 308–312.

83. Qiu RC, Lu I-T. Multipath resolving with frequency dependence for wide-band wireless channel modeling. *IEEE Transactions on Vehicular Technology* 1999; **48**(1): 273–285.
84. Qiu RC. A study of the ultra-wideband wireless propagation channel and optimum UWB receiver design. *IEEE Journal on Selected Areas in Communications* 2002; **20**(9): 1628–1637.
85. Ramirez-Mireles F. On performance of ultra-wideband signals in Gaussian noise and dense multipath. *IEEE Transactions on Vehicular Technology* 2001; **50**(1): 244–249.
86. Ramirez-Mireles F. Performance of ultra wideband SSMA using time hopping and *M*-ary PPM. *IEEE Journal on Selected Areas in Communications* 2001; **19**(6): 1186-1196.
87. Ramirez-Mireles F. Signal design for ultra-wide-band communications in dense multipath. *IEEE Transactions on Vehicular Technology* 2002; **51**(6): 1517–1521.
88. Ramjee R, La Porta T, Thuel S, Varadhan K, Wang SY. HAWAII: a domain-based approach for supporting mobility in wide-area wireless networks. *IEEE/ACM Transactions on Networking* 2002; **10**(3): 396–410.
89. Rappaport TS. *Wireless Communications: Principles and Practices*, Prentice-Hall, 1996.
90. Ross GF. The transient analysis of certain TEM mode four-post networks. *IEEE Transactions on Microwave Theory Technologies* 1966; **14**: 528.
91. Saleh AA, Valenzuela RA. A statistical model for indoor multipath propagation. *IEEE Journal on Selected Areas in Communications* 1987; **5**(2): 128–137.
92. Schantz HG. Radiation efficiency of UWB antennas. *Proceedings of IEEE Conference Ultra-Wideband Systems and Technologies* 2002; 351–355.
93. Scholtz RA. Multiple access with time-hopping impulse modulation. *Proceedings of IEEE MILCOM* 1993; **2**: 447–450.
94. Scholtz RA. Answers to questions posed by Bob Lucky, Chairman of the FCC's Technical Advisory Committee (e-mail correspondence). http: //ultra.usc.edu/ulab June1999.
95. Scholtz RA, Win MZ, Cramer RJ. Evaluation of the characteristics of the ultra-wideband propagation channel. *Proceeding Antennas and Propagation Society International Symposium* 1998; **2**: 626–630.
96. Schwartz M. *Broadband Integrated Networks*. Prentice-Hall: Upper Saddle River, New Jersey, 1996.
97. Siwiak K. Ultra-wide band radio: introducing a new technology. *Proceedings of IEEE VTC* 2001; 1088–1093.
98. Sobrinho JL, Krishnakumar AS. Quality-of-service in ad hoc carrier sense multiple access wireless networks. *IEEE Journal on Selected Areas in Communications* 1999; **17**(8): 1353–1368.
99. Soleimanipour M, Zhuang W, Freeman GH. Optimal resource management in wireless multimedia wideband CDMA systems. *IEEE Transactions on Mobile Computing* 2002; **1**(2): 143–160.
100. Dorte DD, Femminella M, Reali G, Zeisberg S. Network service provisioning in UWB open mobile access networks. *IEEE Journal on Selected Areas in Communications* 2002; **20**(9): 1745–1753.
101. Taha A, Chugg K. Multipath diversity reception of wireless multiple access time-hopping digital impulse radio. *Proceedings of IEEE Conference on Ultra-Wideband Systems and Technologies* 2002; 283–288.
102. Taniguchi T, Kobayashi T. An omnidirectional and low VSWR antenna for ultra-wideband wireless systems. *Proceedings of IEEE RAWCON* 2002; 145–148.
103. Taylor JD. *Ultra-Wideband Radar Technology.* CRC Press: New York, 2001.
104. Taylor JD. *An Introduction to Ultra-Wideband Radar Technology.* CRC Press: Boca Raton, FL, 1995.
105. Turin GL, *et al.* A statistical model for urban multipath propagation. *IEEE Transactions on Vehicular Technology* 1972; **21**(1): 1–9.
106. Uguen B, Plouhinec E, Lostanlen Y, Chassay G. A deterministic ultra wideband channel modeling. *Proceedings of IEEE Conference on Ultra-Wideband Systems and Technologies* 2002; 1–5.
107. United States Code of Federal Regulations, Title 47, Part 15, Subpart 209, U.S. Government Printing Office, http://www.access.gpo.gov/nara/cfr/index.html.
108. van Stralen N, Dentinger A, Welles K, II, Gaus R, Jr, Hoctor R, Tomlinson H. Delay hopped transmitted reference experimental results. *Proceedings of IEEE Conference on Ultra-Wideband Systems and Technologies* 2002; 93–98.
109. Van't Hof JP, Stancil DD. Ultra-wideband high data rate short range wireless links. *Proceeding of IEEE VTC* 2002; 85–89.
110. Verdu S. *Multiuser Detection*. Cambridge University Press: New York, 1998.
111. Welborn M, McCorkle J. The importance of fractional bandwidth in ultra-wideband pulse design. *Proceedings of IEEE ICC* 2002; **2**: 753–757.
112. Welborn M, Miller T, Lynch J, McCorkle J. Multi-use perspectives in UWB communications networks. *Proceedings of IEEE UWBST* 2002; 271–275.
113. Welch TB, Musselman RL, Emessiene BA, Gift PD, Choudhury DK, Cassadine DN, Yano SM. The effects of the human body on UWB signal propagation in an indoor environment. *IEEE Journal on Selected Areas in Communications* 2002; **20**(9): 1778–1782.
114. Win MZ. A unified spectral analysis of generalized time-hopping spread-spectrum signals in the presence of timing jitter. *IEEE Journal on Selected Areas in Communications* 2002; **20**(9): 1664–1676.
115. Win MZ, Scholtz RA. Characterization of ultra-wide bandwidth wireless indoor channels: a communication-theoretic view. *IEEE Journal on Selected Areas in Communications* 2002; **20**(9): 1613–1627.
116. Win MZ, Scholtz RA. Ultra-wide bandwidth time-hopping spread-spectrum impulse radio for wireless-access communications. *IEEE Transactions on Communications* 2000; **48**(4): 679–691.
117. Win MZ, Scholtz RA. Impulse radio: how it works. *IEEE Communications Letters* 1998; **2**(2): 36–38.
118. Win MZ, Scholtz RA. On the robustness of ultra-wide bandwidth signals in dense multipath environments. *IEEE Communications Letters* 1998; **2**(2): 51–53.
119. Win MZ, Scholtz RA, Barnes MA. Ultra-wide bandwidth signal propagation for indoor wireless communications. *Proceedings of IEEE ICC* 1997; **1**: 56–60.
120. Wu S, Wong KYM, Li B. A dynamic call admission policy with precise QoS guarantee using stochastic control for mobile wireless networks. *IEEE Transactions on Networking* 2002; **10**(2): 257–271.
121. Yang L, Hanzo L. Residue number system assisted fast frequency-hopped synchronous ultra-wideband spread-spectrum multiple access: a design alternative to impulse radio. *IEEE Journal on Selected Areas in Communications* 2002; **20**(9): 1652–1663.
122. Yano SM. Investigating the ultra-wideband indoor wireless channel. *Proceeding of IEEE VTC* 2002; 1200–1204.
123. Yoon YC, Kohno R. Optimum multi-user detection in ultra-wideband (UWB) multiple access communications systems. *Proceedings of IEEE ICC* 2002; **2**: 812–816.
124. Zhang H, Udagawa T, Arita T, Nakagawa M. Home entertainment network: combination of IEEE 1394 and ultra wideband solutions. *Proceedings of IEEE Conference Ultra-Wideband Systems and Technologies* 2002; 141–145.
125. Zhao L, Haimovich AM. Performance of ultra-wideband communications in the presence of interference. *IEEE Journal*

on Selected Areas in Communications 2002; **20**(9): 1684–1691.

126. Zhao D, Shen X, Mark JW. Radio resource management for cellular CDMA systems supporting heterogeous services. *IEEE Transactions on Mobile Computing* (to appear).

Authors' Biographies

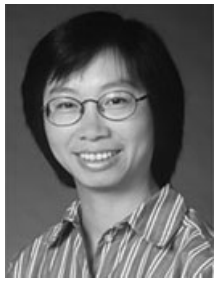

Weihua Zhuang received the B.Sc. and M.Sc. degrees from Dalian Marine University, China, in 1982 and 1985, respectively, and was awarded Ph.D. from the University of New Brunswick, Canada, in 1993, in Electrical Engineering. Since October 1993, she has been with the Department of Electrical and Computer Engineering, University of Waterloo, Ontario, Canada, as a professor. She is a co-author of the textbook *Wireless Communications and Networking* (Prentice-Hall, Upper Saddle River, New Jersey, USA, 2003). Her current research interests include multimedia wireless communications, wireless networks and radio positioning. Dr. Zhuang is a senior member of the IEEE, and a licensed professional engineer in the Province of Ontario, Canada. She received the Premier's Research Excellence Award (PREA) in 2001 from the Ontario Government for demonstrated excellence of scientific and academic contributions.

Xuemin (Sherman) Shen received the B.Sc. (1982) degree from Dalian Marine University (China) and the M.Sc. (1987) and was awarded Ph.D. (1990) from Rutgers University, New Jersey (USA), in Electrical Engineering. From September 1990 to September 1993. He was first with Howard University, Washington DC and then University of Alberta, Edmonton (Canada). Since October 1993, he has been with the Department of Electrical and Computer Engineering, University of Waterloo, Canada, where he is a full professor. Dr. Shen's research focuses on mobility and resource management in interconnected wireless/wireline networks, stochastic process and control. He is a co-author of two books and has publications in communications networks, control and filtering. Dr. Shen received the Premier's Research Excellence Award (PREA) in 2003 from the Province of Ontario for demonstrated excellence of scientific and academic contributions, and the Distinguished Performance Award in 2002 from the Faculty of Engineering, University of Waterloo, for outstanding contribution in teaching, scholarship and service. He serves as the Technical Vice Chair, IEEE Globecom'03 Symposium on Next Generation Networks and Internet; the Editor, *Dynamics of Continuous, Discrete and Impulse Systems, Series B*: *Application and Algorithm*—an International Journal; and the Technical Program Vice Chair, International Symposium on Parallel Architectures, Algorithms, and Networks. Dr. Shen is a senior member of the IEEE, and a registered professional engineer of Ontario, Canada.

Qi Bi received his B.S. and M.S. from the Shanghai Jiao Tong University in 1978 and 1981, and was awarded Ph.D. from the Pennsylvania State University in 1986. He joined the Bell Labs as a member of technical staff in 1988, was awarded the Distinguished Member of Technical Staff in 1995 and became a technical manager in 1997. Dr. Qi Bi was the recipient of numerous honours including the Advanced Technologiesogy Laboratory Award of 1995, the Advanced Technologiesogy Laboratory Awards of 1996, the Bell Labs President's Gold Award 2000, guest Professor of Shanghai Jiao Tong University in 2000 and the Bell Labs President's Gold Award 2002. In 2002, he was awarded the prestigious Bell Labs Fellow 'for his pioneering contributions in analysis, design and optimization of CDMA systems that resulted in Lucent Technologiesogies' global success in digital wireless communications'.

Dr. Bi is also an active leader in his areas of expertise. He served as either the technical chair or the vice chair in many international conferences including: 3G Wireless Symposium 2003, IEEE Wireless Communications and Network Conference 2003, Wireless Symposium of IEEE Globecom 2002, 3G Wireless 2002, Wireless Symposium of IEEE Globecom 2001, International Conference on Wireless Internet Technologies 2001, 3G Wireless Conference 2001, International Conference on Broadband Wireless Access 2001, Wireless Broadband Symposium of IEEE Globecom 2000, 3G Wireless Conference 2000, Organizer of The 2nd Lucent IS-95 & UMTS Technical Conference in 2000, Organizer of The 1st Lucent IS-95 & UMTS Technical Conference in 1999, Wireless Mobile ATM Conference 1999, and Wireless Mobile ATM Conference 1998. He also served or is serving as the guest editor of *Wireless Communications and Mobile Computing* from Wiley, Feature Editor of *IEEE Communications Magazine*, 2001, Editor of *IEEE Journal on Selected Areas in Communications* and the Editor of *IEEE Transaction on Wireless Communications*. Dr. Bi holds more than 20 US patents, and has published many Journal and Conference papers. He was listed in Who's who in America, and featured in Bund Magazine in 8 November 2002.